Mixture of ligands influence on metal accumulation in Diffusive Gradients in Thin films (DGT)

Journal:	*Environmental Chemistry*
Manuscript ID	Draft
Manuscript Type:	Research paper
Date Submitted by the Author:	n/a
Complete List of Authors:	Altier, Alexandra; Universitat de Lleida, Departament de Quimica Jimenez-Piedrahita, Martin; Universitat de Lleida, Departament de Quimica Uribe, Ramiro; Universidad de Tolima, Fisica Rey Castro, Carlos; University of Lleida, Department of Chemistry Cecilia, Joan; Universitat de Lleida, Departament de Matemàtica Galceran, Josep; Universitat de Lleida, Departament de Quimica Puy, Jaume; Universitat de Lleida, Departament de Quimica
Keyword:	Speciation, Trace metals, Bioavailability, Kinetic modelling

This work analyses the influence of the composition of the system on the availability of metal cations as nutritive or toxic species. The main question that tries to clarify is whether the availability measured in single ligand systems with the Diffusive Gradients in Thin Film (DGT) devices can be used to predict the contribution of each complex in the mixtures. A new interaction mechanism by which partially labile complexes become more inert in presence of a labile complex is reported. Although all natural systems are large mixtures, mixture effects have not received until recently great interest.

Mixture of ligands influence on metal accumulation in Diffusive Gradients in Thin films (DGT)

Alexandra Altier[a], Martín Jiménez-Piedrahita[a], Ramiro Uribe[c], Carlos Rey-Castro[a], Joan Cecília[b], Josep Galceran[a], Jaume Puy[a*]

[a]*Departament de Química.* [b]*Departament de Matemàtica. Universitat de Lleida, and AGROTECNIO, Rovira Roure 191, 25198 Lleida, Catalonia, Spain;* [c]*Department of Physics, University of Tolima, Colombia*

* Corresponding author, email address: jpuy@quimica.udl.cat, Phone 34 973 702529, Fax 34 973 702924

Abstract

Natural waters contain mixtures of ligands, which collectively affect the availability of trace metals. The individual contribution of each complex to the overall metal flux received by a sensor can be described in terms of its lability degree. The question arises as to whether the mixture entails specific non-additive effects, *i.e*. to what extent is it possible to predict the collective behaviour of the mixture from the values of the lability degrees of each single ligand system (SLS). For this reason, a series of experiments with DGT (Diffusion Gradients in Thin films) devices were carried out to measure nickel accumulations from synthetic media comprising either Nitrilotriacetic acid (NTA), Ethylenediamine (EN) or mixtures of both ligands. The results were compared with numerical simulations.

It is shown that NiEN and NiNTA can become more labile and inert (respectively) in the mixture than in the corresponding SLS. This unprecedented behaviour arises when one of the ligands (NTA, forming strong and partially labile complexes) is present at non-excess conditions ($c^*_{ML} >> c^*_L$, $c^*_{ML} >> c^*_M$). As variations in the lability degrees of NiNTA and NiEN arising in the mixture tend to cancel out, the summation of partial

fluxes calculated from lability degrees obtained in SLS yields a reasonable estimate of the DGT performance in the mixture. Experimental accumulations in the mixture are just slightly below the predicted values, with errors lower than 11 % within a range of NTA concentrations equivalent to 20% - 100% of the total Ni concentration.

Keywords: DGT, lability degree, diffusion coefficients, mixture effects

1. Introduction

Natural waters contain mixtures of metal cations and ligands whose interactions largely determine the availability of the former to biota and plants[1-6]. The metal uptake flux, i. e., the supplied flux to the surface of interest is, in general, the most meaningful measurement to assess availability. As ligand concentrations are usually orders of magnitude more abundant than those of trace metals, the availability of metals is, typically, determined by the ability of complexes to dissociate in the pertinent time and spatial scales. The lability degree was introduced as a way to quantify the contribution of an individual complex to the overall metal flux[7-9] It is the fraction of the current contribution of the complex to the metal flux with respect to the maximum contribution that would arise if dissociation was so fast as to instantaneously reach equilibrium at any relevant spatial position. In single ligand systems (SLS), the lability degree can straightforwardly be measured as a kind of normalized flux, avoiding the use of numerical fitting procedures[10]. However, the lability degree has the drawback that it is not an intrinsic property of the complex, but it is also dependent on the sensor characteristics and the composition of the system[11,12]. Previous works on voltammetric sensors under steady state conditions have shown [13-15] that the addition of labile ligands to the system tends to increase the lability degree of the more inert complexes, whereas the addition of inert ligands tends to decrease the lability degree of labile complexes.

Buffle and co-workers[16,17] reported that the metal fux can be orders of magnitude diferent from what expected when the flux in the mixture is computed with the lability degrees of single ligand systems. We refer to "mixture effect" to indicate a change in the flux contribution of one metal-ligand complex due to the presence of other ligands also complexing the same metal when the SLS and the mixture share identical concentrations of free metal, ligand and complex. In a mixture of several complexes, there might be a relevant difference in the total flux with respect to the expected value obtained by direct addition of fluxes measured in the equivalent set of SLS's. The mixture effect is called synergistic when the real flux in the mixture is greater than the expected value obtained from the ensemble of individual SLS's, while it is antagonistic in the opposite case.

In DGT[18,19], complex penetration into the resin disc has a large impact on the reaction layer thickness and the lability degree of complexes[20,21] rendering them more labile than in voltammetric measurements. Besides, the influence of the ligand concentration on the lability degree of a complex in DGT has proved to be almost negligible in conditions of excess of ligand, since most of the complex dissociation takes place in the resin domain, where the net rate of dissociation cannot be influenced by a variable amount of ligand due to the absence of free metal [22]. Consequently, the error in using lability degrees measured in SLS to assess the accumulation in complex mixtures has been quantified as being less than 10% in systems with a couple of complexes and it is further reduced to 4% when a doble resin disc is used in the DGT device [23].

However, all this previous work has been done under excess of ligand conditions which could not be valid in some practical situations. A system with Ni, NTA and EN at pH 8 and salt background 50 mol m^{-3} is used in this work as a case study. The theoretical framework and experimental details are reported in Sections 1 and 2, respectively.

Separate experiments for the corresponding single ligand systems are run to determine the corresponding lability degrees in Sections 3.1 and 3.2. Section 3.3 is devoted to the behaviour of the mixture. It is concluded that the metal accumulation in the mixture system can be reasonably predicted from the lability degree values measured in the corresponding SLS's at the same free ligand concentration.

2. The lability degree

2.1 Single ligand systems (SLS)

Let us consider the SLS where the metal M binds to the ligand L to form the complex ML

$$\mathrm{M} + \mathrm{L} \underset{k_\mathrm{d}}{\overset{k_\mathrm{a}}{\rightleftharpoons}} \mathrm{ML} \qquad (1)$$

where k_a and k_d are the association and dissociation rate constants, respectively.

Under steady-state conditions, the flux of the metal bound to the resin disc, J, results from the contributions of free M in solution and complex ML,

$$J = J_\mathrm{free} + J_\mathrm{lab}\xi \qquad (2)$$

where, for DGT,

$$J_\mathrm{free} = D_\mathrm{M}\frac{c_\mathrm{M}^*}{\delta^g} \qquad (3)$$

is the contribution to the flux of the free M in solution,

$$J_\mathrm{lab} = D_\mathrm{ML}\frac{c_\mathrm{ML}^*}{\delta^g} \qquad (4)$$

is the maximum contribution of the complex, arising when dissociation is fast enough to reach equilibrium with the metal in all the diffusive gel domain. ξ stands for the lability degree [7], D_i and c_i^* label the diffusion coefficient and the bulk concentration of species i, respectively, and δ^g includes the thicknesses of the diffusive gel, the filter membrane

and the diffusive boundary layer (DBL), where a common diffusion coefficient for each species is assumed.

For single ligand systems, ξ is easily measured as a normalized flux [10,24], once J_{free} has been subtracted. For instance, when J_{free} is negligible, the lability degree can be computed as,

$$\xi \equiv \frac{J}{J_{\text{labile}}} = \frac{n_{\text{M}}/At}{D_{\text{ML}}\left(\frac{c^{*}_{\text{ML}}}{\delta^{g}}\right)} \tag{5}$$

where n_{M} is the number of moles of M accumulated in the resin in a deployment time t and A is the effective area of the gel-solution interface.

2.2 Lability degree in a mixture of ligands

Let us consider a metal M that can be bound to several ligands ^{1}L, ^{2}L…^{h}L according to the parallel scheme of reactions,

$$\text{M} + {}^{i}\text{L} \underset{k_{\text{d},i}}{\overset{k_{\text{a},i}}{\rightleftharpoons}} \text{M}^{i}\text{L} \qquad i = 1, 2, \ldots, h \tag{6}$$

where subscript i indicates that the parameters correspond to the complexation with ^{i}L. When the resin acts as a perfect sink for the metal, the flux of metal accumulated by the resin becomes[10,23] $J = J_{\text{free}} + \sum_{i=1}^{h} J_{\text{M}^{i}\text{L,lab}}\xi_{\text{M}^{i}\text{L}}$ (7)

where $\xi_{\text{M}^{i}\text{L}}$ labels the lability degree of each complex in the mixture defined as

$$\xi_{\text{M}^{i}\text{L}} \equiv 1 - \frac{c^{\text{r}}_{\text{M}^{i}\text{L}}}{c^{*}_{\text{M}^{i}\text{L}}} \tag{8}$$

$c^{\text{r}}_{\text{M}^{i}\text{L}}$ stands for the complex concentration at the resin/diffusive gel interface and $J_{\text{M}^{i}\text{L,lab}}$ is given by Eqn. (4). Given the definition, $\xi_{\text{M}^{i}\text{L}}$ is hardly measurable since only the total accumulation of M coming from the whole ensemble of metal complexes is measured in

DGT. However, the estimation of ξ_{M^iL} in the single ligand system and a suitable correction to account for the mixture effect, if necessary, can open the way to study mixtures from measurements in simple systems. Additionally, this procedure could also serve to identify synergistic or antagonistic effects in the mixture.

3. Experimental

3.1 Test solutions

Solutions of Ni, with either the strong chelating ligand nitrilotriacetic Acid (NTA, Fluka, analytical grade) or ethylenediamine (EN) (Fluka), were used as single ligand systems or in a mixture.

A 10 mol·m^{-3} solution of Ni was prepared as stock solution from the corresponding metal nitrate salt ($Ni(NO_3)_2 \cdot 6H_2O$, Sigma Aldrich). Sodium nitrate, $NaNO_3$ (Sigma-Aldrich, puriss p.a.), was used as background electrolyte to fix the ionic strength (I) at 50 mol m^{-3}. Buffered solutions were obtained with 1 mol m^{-3} HEPES (4-(2-hydroxyethyl)-1-piperazineethanesulfonic acid) at pH 8, adjusted by dropwise addition of 10^3 mol·m^{-3} NaOH or HNO_3 (Fluka). HEPES complexation of Ni ions is assumed to be negligible [25,26].

Three separately experiments were conducted at the conditions specified in Table 1. These experimental conditions were selected in order to have a negligible free metal concentration to better identify the lability change of complexes, while none of the contributions of the complexes was negligible. Additionally, concentrations in the SLS were chosen to have similar bulk free metal and free ligand concentrations to those of the mixture (especially for the Ni+NTA system) as explained in Section 3.3.2 (see the SI for the speciation calculation of these solutions according to Visual MINTEQ[27]).

3.2 DGT deployments

DGT devices (piston type, 2 cm diameter window), acrylamide cross-linked with and agarose derived gel discs (diffusive disc, 0.8 mm thick, and Chelex resin disc, 0.4 mm thick) and cellulose nitrate membrane filters (0.45 µm pore size, 0.125 mm thick) were used.

In order to obtain additional information on the spatial distribution of the accumulated Ni, DGT devices with two resin discs (front, F, close to the diffusive gel and back, B, at the bottom of the sensor) were used. The accumulated Ni in each resin disc was separately determined from their acid-eluted solutions via analysis with inductively coupled plasma mass spectrometry (ICP-MS, 7700 Series, Agilent).

2.3 Parameters

The values of the diffusion coefficients at 25 ºC used in calculations are 6.08×10^{-6} cm^2s^{-1} [1] for Ni, as reported by Shiva *et al.* [28], 4.75×10^{-6} cm^2s^{-1} for NiNTA and NTA, which correspond to 0.78 times the value of the free metal ions [29], and 6.08×10^{-6} cm^2s^{-1} for the NiEN complexes and EN ligand. A common value with D_{Ni} was chosen for the latter species, since accumulations of different metals in a solution with EN do not show dependence on the stoichiometric metal-to-ligand ratio of the complex species formed (See table SI-9). The effective area used is $A = 3.14\times10^{-4}$ m^2 and $\delta^g = 1.1\times10^{-3}$ m.

4. Results and discussion

4.1 Lability degree of the NiNTA complex in the SLS

4.1.1 Ni+NTA system

Experimental values of the total accumulation in the resin as well as the percentage accumulated in the back resin (calculated from the number of moles eluted from back and front resins) at different deployment times (see Table 2) were obtained for a system

171 with Ni and NTA at the concentrations indicated in Table 1. At these conditions, the
172 main reactions in this system are:

173 $$\mathrm{Ni} + \mathrm{NTA} \underset{k_{\mathrm{d,NiNTA}}}{\overset{k_{\mathrm{a,NiNTA}}}{\rightleftharpoons}} \mathrm{NiNTA} \quad (9)$$

174 $$\mathrm{H} + \mathrm{NTA} \underset{k_{\mathrm{d,HNTA}}}{\overset{k_{\mathrm{a,HNTA}}}{\rightleftharpoons}} \mathrm{HNTA} \quad (10)$$

175

176 Additionally, Ni can be accumulated in the resin domain. Assuming that protonation
177 reactions are fast enough to consider that equilibrium is instantaneously reached at any
178 spatial position and assuming that the diffusion of protons is so fast that there is a
179 homogeneous proton concentration profile, the mathematical formulation of the system
180 Ni+NTA can be reduced to a system where Ni reacts with only one formal species that
181 can be called effective ligand $\mathrm{NTA}^{\mathrm{eff}}$ as:

182 $$\mathrm{Ni} + \mathrm{NTA}^{\mathrm{eff}} \underset{k^{\mathrm{eff}}_{\mathrm{d,NiNTA}}}{\overset{k^{\mathrm{eff}}_{\mathrm{a,NiNTA}}}{\rightleftharpoons}} \mathrm{NiNTA} \quad (11)$$

183 With:

184 $$c^{\mathrm{eff}}_{\mathrm{NTA}} = c_{\mathrm{NTA}} + c_{\mathrm{HNTA}} \quad (12)$$

185 Where:

186 $$k^{\mathrm{eff}}_{\mathrm{a,NiNTA}} = \frac{k_{\mathrm{a,NiNTA}}}{1 + K_{\mathrm{HNTA}} c_{\mathrm{H}}} \quad (13)$$

187 $$k^{\mathrm{eff}}_{\mathrm{d,NiNTA}} = k_{\mathrm{d,NiNTA}} \quad (14)$$

188 $$K^{\mathrm{eff}}_{\mathrm{NiNTA}} = \frac{k^{\mathrm{eff}}_{\mathrm{a,NiNTA}}}{k^{\mathrm{eff}}_{\mathrm{d,NiNTA}}} \quad (15)$$

189 See the supporting information (SI) for details of this formulation. In this way, the
190 Ni+NTA system can be analysed in the framework of the simple scheme represented by
191 Eqn. (1).

The high percentage of Ni accumulated in the back resin disc (Table 2) indicates that NiNTA is not fully labile in DGT [31,32]. According to the speciation distribution predicted by Visual MINTEQ for the conditions summarized in Table 1, the free Ni concentration is negligible (see Table SI-2). The lability degree of the NiNTA complex in the SLS (labelled as $\xi^{h=1}_{\mathbf{NiNTA}}$) was, therefore, calculated using Eqn. (5) and reported in Table 2.

The knowledge of the dependence of $\xi^{h=1}_{\mathbf{NiNTA}}$ on the composition of the system facilitates the assessment of $\xi^{h=1}_{\mathbf{NiNTA}}$ at the desired concentrations of the mixture. To this knowledge is devoted the next Section 3.1.1.

4.1.2 Dependence of the lability degree of NiNTA on NTA concentration

Values for the effective kinetic constants of the system Ni+NTA, defined in Eqns. (13) and (14), were estimated using numerical simulation to fit the experimental data reported in Table 2a. Retrieved values are reported in Table 3, while details of the fitting procedure can be found in the SI. With these constants, we can assess, by simulation, the variation of the lability degree of the NiNTA in the SLS with NTA concentration. This dependence is depicted in Figure 1, where the calculated labilities are plotted as a function of the total (Figure 1a) or the effective ligand (Figure 1b) concentrations.

In conditions of a relative excess of ligand, where $c^{*}_{\mathrm{T,NTA}} > c^{*}_{\mathrm{T,Ni}}$ ($c^{*}_{\mathrm{T},i}$ stands for the total concentration of species *i*), the lability degree tends to a constant value and becomes independent of the NTA concentration. This behaviour was previously predicted for DGT measurements [23] and it indicates that almost all metal accumulation comes from dissociation of the complex in the resin domain where the shift of reaction (1) towards association is negligible due to the absence of free metal.

On the other hand, in the non-excess regime ($c^*_{T,NTA} < c^*_{T,Ni}$), the value of $\xi^{h=1}_{NiNTA}$ decreases as $c^*_{T,NTA}$ decreases. To understand this behaviour we point out that, when ligand excess conditions are not valid, the ligand concentration profile along the DGT device is not flat. Instead, the local NTA concentration increases as we move from the bulk solution to the resin/diffusive gel interface, as Figure 2b shows for the bulk concentrations reported in Table 1. The slope of the normalized NTA concentration profile indicates that there is a net flux of NTA from the resin towards the diffusive gel to maintain steady-state conditions and to compensate for the release of NTA from the dissociation of the complex in the resin domain.

The increased ligand concentration (Figure 2b) that both, the free metal (Figure 2c) and the complex (Figure 2a) encounter in their diffusion towards the resin disc, leads to a shift of the complexation process towards association. As the bulk concentration of ligand becomes progressively lower ($c^*_{T,NTA} \ll c^*_{T,Ni}$), the concentration profile of the ligand within the diffusion domain grows steeper and, accordingly, the lability degree of the complex decreases (as shown in Figure 1a).

Finally, Figure 1b shows that $\xi^{h=1}_{NiNTA}$ values for different $c^*_{T,Ni}$ and $c^*_{T,NTA}$ virtually collapse to a common curve when these data are plotted in front of c^{eff*}_{NTA}, which indicates the importance of controlling the bulk concentration of the free ligand to have a desired value of the lability degree. Abscissae values corresponding to $c^*_{T,Ni} = c^*_{T,NTA}$ are indicated in Figure 1b as vertical dotted lines. Notice that there is a wide range of free ligand concentrations around this equimolar composition where $\xi^{h=1}_{NiNTA}$ remains approximately constant and equal to the value in the ligand-excess regime. This range includes the concentrations of Ni and NTA reported in Table 1. The lower bound value

of this range can be approximately estimated as follows. Notice that, for any Ni to NTA ratio, the steady-state profile of $c_{\mathrm{T,NTA}}$ is flat (except for a step discontinuity at the resin/diffusive gel interface of electrostatic origin, as explained below), since there is no net consumption of NTA anywhere in the system. Therefore, it can be shown that, in steady-state, $c_{\mathrm{T,NTA}}(x) = c_{\mathrm{NiNTA}}(x) + c_{\mathrm{NTA}}^{\mathrm{eff}}(x) \approx c_{\mathrm{T,NTA}}^{*}$ throughout the gel disc. Consequently, the decrease in c_{NiNTA} due to dissociation at the resin-gel interface implies an equivalent increase in $c_{\mathrm{NTA}}^{\mathrm{eff}}$ at this point ($c_{\mathrm{NTA}}^{\mathrm{eff}}\left(x=\delta^{\mathrm{r}}\right) - c_{\mathrm{NTA}}^{*\mathrm{eff}} = c_{\mathrm{NiNTA}}^{*} - c_{\mathrm{NiNTA}}\left(x=\delta^{\mathrm{r}}\right)$, a condition that can also be rewritten as $c_{\mathrm{NiNTA}}^{*} - c_{\mathrm{NiNTA}}\left(x=\delta^{\mathrm{r}}\right) = \xi_{\mathrm{NiNTA}}^{h=1} c_{\mathrm{NiNTA}}^{*}$ according to (Eqn. 8)). This increase will impact on $\xi_{\mathrm{NiNTA}}^{h=1}$ whenever there is enough free Ni to be complexed with this extra NTA concentration in the diffusion domain, i. e., when $\xi_{\mathrm{NiNTA}}^{h=1} c_{\mathrm{NiNTA}}^{*}$ is of the order of the free metal concentration, $\xi_{\mathrm{NiNTA}}^{h=1} c_{\mathrm{NiNTA}}^{*} \approx c_{\mathrm{Ni}}^{*}$. For a strong complex and a total ligand/metal ratio lower than 1, $c_{\mathrm{NiNTA}}^{*} \approx c_{\mathrm{T,NTA}}^{*}$, the condition $\xi_{\mathrm{NiNTA}}^{h=1} c_{\mathrm{NiNTA}}^{*} \approx c_{\mathrm{Ni}}^{*}$ can be approximately rewritten as $\xi_{\mathrm{NiNTA}}^{h=1} c_{\mathrm{T,NTA}}^{*} \approx c_{\mathrm{T,Ni}}^{*} - c_{\mathrm{T,NTA}}^{*}$, i. e.,

$$c_{\mathrm{T,NTA}}^{*} \approx \frac{1}{1+\xi_{\mathrm{NiNTA}}^{h=1}} c_{\mathrm{T,Ni}}^{*} . \qquad (16)$$

Using $\xi_{\mathrm{NiNTA}}^{h=1} \approx 0.6$ from Figure 1, this expression yields $c_{\mathrm{T,NTA}}^{*} \approx 0.625 c_{\mathrm{T,Ni}}^{*}$ indicating that for $c_{\mathrm{T,NTA}}^{*} > 0.625 c_{\mathrm{T,Ni}}^{*}$ the lability degree of NiNTA is close to the value in ligand excess conditions. This means that, given a $c_{\mathrm{T,Ni}}^{*}$, we have a range of $c_{\mathrm{T,NTA}}^{*}$ values below $c_{\mathrm{T,Ni}}^{*}$ where the variation of $\xi_{\mathrm{NiNTA}}^{h=1}$ is negligible and, so the experimental

measurement of $\xi_{\mathrm{NiNTA}}^{h=1}$ becomes less restricted to match exactly the conditions in the mixture. Figure 1b indicates that this range spans more than one order of magnitude in terms of $c_{\mathrm{NTA}}^{\mathrm{eff}*}$. Around this limit, i. e, for $c_{\mathrm{T,NTA}}^{*} \sim 0.625 c_{\mathrm{T,Ni}}^{*}$, $\xi_{\mathrm{NiNTA}}^{h=1}$ is strongly dependent on the $c_{\mathrm{NTA}}^{\mathrm{eff}*}$ and the experimental measurement would require the accurate preparation of a system with the prescribed free metal, free ligand and complex concentrations.

As anticipated above, the ligand and complex concentration profiles show a step discontinuity at the resin layer/diffusive gel interface (Figures 2a and 2b). This is due to electrostatic effects[33-37], which -in this case- tend to exclude negatively charged mobile species from the Chelex resin phase. In order to quantitatively account for this effect in the numerical simulations, the Boltzmann factor corresponding to this pH and salt background was experimentally determined by adding a small amount of Rb into the solution and measuring the ratio of Rb concentrations between resin and diffusive gels. Rb, as well as Na, are assumed to have a negligible intrinsic chemical binding with the resin sites, so that concentrations in the resin domain over the bulk concentration correspond to electrostatic accumulations [33]. At pH 8 and ionic strength 500 mol·m^{-3}, a partitioning (or Boltzmann) factor $\Pi_{\mathrm{Rb}} = \dfrac{c_{\mathrm{Rb}}\left(x=\delta^{r^-}\right)}{c_{\mathrm{Rb}}\left(x=\delta^{r^+}\right)} = 2$ was obtained, so that $\dfrac{c_{\mathrm{NTA}}\left(x=\delta^{r^-}\right)}{c_{\mathrm{NTA}}\left(x=\delta^{r^+}\right)} = \Pi_{\mathrm{Rb}}^{z_{\mathrm{NTA}}} = \dfrac{1}{2^3}$. Discontinuities for all the other charged species are also observed, with the ratio of concentrations being $\dfrac{c_i\left(x=\delta^{r^-}\right)}{c_i\left(x=\delta^{r^+}\right)} = \Pi_{\mathrm{Rb}}^{z_i}$.

4.2 Lability degree of the NiEN complexes in the SLS

There are complexes of Ni and EN with stoichiometric metal-to-ligand ratios from 1:1 to 1:3. Thus, the following set of reactions has to be considered

$$\mathrm{Ni} + \mathrm{EN} \underset{k_{\mathrm{d,NiEN}}}{\overset{k_{\mathrm{a,NiEN}}}{\rightleftharpoons}} \mathrm{NiEN} \quad (17)$$

$$\mathrm{NiEN} + \mathrm{EN} \underset{k_{\mathrm{d,Ni(EN)_2}}}{\overset{k_{\mathrm{a,Ni(EN)_2}}}{\rightleftharpoons}} \mathrm{Ni(EN)_2} \quad (18)$$

$$\mathrm{Ni(EN)_2} + \mathrm{EN} \underset{k_{\mathrm{d,Ni(EN)_3}}}{\overset{k_{\mathrm{a,Ni(EN)_3}}}{\rightleftharpoons}} \mathrm{Ni(EN)_3} \quad (19)$$

$$\mathrm{H} + \mathrm{EN} \underset{k_{\mathrm{d,HEN}}}{\overset{k_{\mathrm{a,HEN}}}{\rightleftharpoons}} \mathrm{HEN} \quad (20)$$

$$\mathrm{H} + \mathrm{HEN} \underset{k_{\mathrm{d,H_2EN}}}{\overset{k_{\mathrm{a,H_2EN}}}{\rightleftharpoons}} \mathrm{H_2EN} \quad (21)$$

Additionally, Ni reacts with the resin sites. Association and dissociation kinetic constants were estimated using numerical simulation to fit the experimental Ni accumulation data presented in Table 2b. In the fitting, it was assumed that protonation is a fast process (so that it instantaneously reaches equilibrium), and that all species $\mathrm{Ni(EN)}_i$ are in equilibrium between them for i >1 [38]. The almost negligible accumulation of Ni in the back resin disc reported in Table 2b indicates that the system Ni+EN behaves as a labile system. Accordingly, the accumulation is almost independent of the particular value of the kinetic constant $k_{\mathrm{d,NiEN}}$ above a threshold value, and, thus, the lowest value approaching the accumulation within a 2% discrepancy was selected. Additionally, the stability constants (as reported in Visual MINTEQ) were used (see Table 3). Details of the fitting procedure as well as values of the kinetic and stability constants are reported in the supporting information.

The specific lability degree of each $\mathrm{Ni(EN)}_i$ complex species can be theoretically established based on its particular dissociation at the resin/gel interface, according to Eq. (8), once the association and dissociation kinetic constants have been fitted. However, since the experimental setup for this ligand uses excess of ligand conditions,

assuming that protonation is a fast process (so that it instantaneously reaches equilibrium), and assuming that $Ni(EN)_i$ are in equilibrium between them for i >1, the global system can also be reduced to a simpler equivalent system: [30]

$$Ni + EN^{eff} \underset{k_{d,NiEN}^{eff}}{\overset{k_{a,NiEN}^{eff}}{\rightleftharpoons}} NiEN^{eff} \quad (22)$$

with:

$$c_{EN}^{eff} = c_{EN} + c_{HEN} + c_{H_2EN} \quad (23)$$

$$c_{NiEN}^{eff} = c_{NiEN} + c_{Ni(EN)_2} + c_{Ni(EN)_3} \quad (24)$$

$$k_{a,NiEN}^{eff} = \frac{k_{a,NiEN}}{1 + K_{HEN}c_H + K_{HEN}K_{H_2EN}c_H^2} \quad (25)$$

$$k_{d,NiEN}^{eff} = \frac{k_{d,NiEN}}{1 + \frac{K_{Ni(EN)_2}c_{EN}^{eff}}{1 + K_{HEN}c_H + K_{HEN}K_{H_2EN}c_H^2}} \quad (26)$$

$$K_{NiEN}^{eff} = \frac{k_{a,NiEN}^{eff}}{k_{d,NiEN}^{eff}} \quad (27)$$

Considering this simple equivalent formulation (see details of this formulation the SI), the experimental lability degree of the $NiEN^{eff}$ complex in SLS can be calculated using Eqn. (5). For a solution with composition detailed in column 2 of Table 1, the measurement of ξ, now denoted $\xi_{NiEN^{eff}}^{h=1}$, is also reported in Table 2b. Moreover, the effective kinetic and stability constants calculated according to Eqns. (25-27) from fitted rate constants reported in the SI are presented in Table 3.

According to the results of the preceding Section 3.1.1, the determination of $NiEN^{eff}$ lability degree in the SLS (in principle, at the concentrations of free Ni, free EN^{eff} and $NiEN^{eff}$ in the mixture) is expected to be almost independent of the accurate

reproduction in the SLS of the mixture concentrations for experiments reported in Table 1.

4.3 Ni+NTA+EN system

In this section, a mixed system with Ni, NTA and EN is studied focussing on whether the lability degree of each complex (in a SLS with the same free metal and the corresponding complex and ligand concentrations) can be used to predict the accumulation in the mixture according to Eqn. (7). This procedure could be a very simple way to predict the accumulation in a mixture of ligands and at the same time will evidence the arising of synergistic or antagonistic mixture effects, since the value predicted with Eqn. (7) using the SLS values of the lability degree (*i.e.*: $\xi_{M^iL} = \xi_{M^iL}^{h=1}$) corresponds to the pure additive value without interaction effects due to the mixture.

As starting point, the effect of the mixture composition on the actual lability degree of each complex shall be analysed. The physicochemical parameters (kinetic and stability constants, diffusion coefficients and geometrical characteristics of the DGT devices) retrieved in the above sections to fit the accumulations and back percentages in SLS of Ni+NTA and Ni+EN will be used to predict the accumulations in the mixture by numerical simulation.

4.3.1 Lability degree of metal complexes in the mixture

Figure 3 shows the simulated dependence of the lability degree of NiNTA and $NiEN^{eff}$ on the concentration of NTA (continuous lines) in a mixture where NTA is not in excess with respect to the metal ($c^*_{T,Ni}$=2.5×10^{-2} mol·m^{-3}). The lability degrees of the corresponding SLS's having the same free Ni, effective complex and effective ligand concentrations are also depicted in Figure 3 as markers. Although hardly noticeable, the

lability degrees of the most labile complex, $NiEN^{eff}$, (red triangle markers and lines) are slightly higher in the mixture than in the SLS values, while $\xi_{NiNTA} < \xi_{NiNTA}^{h=1}$ (blue lines and diamond markers), *i. e.*, dissociation of NiNTA is inhibited by the presence of EN in the system. This behaviour, where the mutual influence tends to increase the difference in the labilities of both complexes in the mixture (divergent mutual influence) is opposite to that previously identified for the mixture effect in excess of ligand conditions [23], where labile complexes become more inert and inert complexes become more labile in the mixtures (convergent mutual influence).

The concentration profiles of the effective species in both SLS and mixed systems (see Figure 2) may help to understand how the mixing of ligands influence the lability degrees of the corresponding complexes. For the $Ni+EN^{eff}$ system there is an excess of ligand and, thus, the concentration profile of EN^{eff} is approximately flat (homogeneous) in the resin and in the diffusive gel domains for both SLS and mixture (Figure 2b). In turn, the free Ni concentration profiles are depicted in Figure 2c. In the mixture, the value of free Ni concentration is constrained by the simultaneous presence of both complexes, resulting in an intermediate concentration profile between the individual profiles of Ni in each SLS. Since the normalized concentration of free Ni in the mixture is lower than in the single $Ni+EN^{eff}$ system, the $NiEN^{eff}$ complex will necessarily tend to dissociate in the mixture to increase the free metal profile towards the corresponding one of the SLS. On the other hand, as the free Ni concentration is higher in the mixture than in the single $Ni+NTA$ system, Ni will tend to associate with the free NTA ligand in the mixture. So, the concentration of $NiEN^{eff}(x)$ decreases and the concentration of NiNTA(x) increases in the mixture with respect to the corresponding values in the SLS, as seen in Figure 2a. Consequently, $NiEN^{eff}$ will be more labile ($\xi_{NiEN^{eff}} > \xi_{NiEN^{eff}}^{h=1}$) and

NiNTA will be more inert ($\xi_{\mathrm{NiNTA}} < \xi_{\mathrm{NiNTA}}^{h=1}$) in the mixture than in the respective single ligand systems. In other words, $\mathrm{NiEN}^{\mathrm{eff}}$ acts as a source of Ni, which is complexed to the increasing NTA concentration found when moving from the bulk solution to the resin domain.

The unexpected behaviour of this mixture with respect to a mixture of the same ligands in excess of ligand conditions is due to the particularly small normalized free metal concentrations in the partially labile Ni+NTA SLS system. In excess of ligand conditions, this concentration profile will be above that of the normalized free Ni in the system Ni+EN, so that the same arguments used above will lead to the more labile complex, NiEN, becoming less labile in the mixture and the opposite behaviour for NiNTA. The especially low free metal profile in the Ni+NTA SLS system in the present case is just a consequence of the increasing normalized NTA profile when going from the bulk solution to the resin domain due to the dissociation of NiNTA in the resin. This increase of the ligand is relevant when $c_{\mathrm{ML}}^{*} >> c_{\mathrm{L}}^{*}$, and it is the responsible for the especially small metal profile when $c_{\mathrm{ML}}^{*} >> c_{\mathrm{M}}^{*}$, since the metal travelling from the solution towards the resin becomes increasingly complexed to the increased NTA profile until the local concentration $c_{\mathrm{M}}(x)$ drops to almost zero when $c_{\mathrm{L}}(x) > c_{\mathrm{M}}(x)$ and $Kc_{\mathrm{L}}^{*} >> 1$.

The lability degree values (calculated with the numerical simulation program for the mixed system at the used experimental conditions) are listed in Table 4. These values are consistent with the back accumulations reported in Table 2. Certainly, Ni accumulation on the back resin disc can be seen as essentially coming from the NiNTA dissociation, since this complex is considerably less labile than NiEN. Whereas in the

399 Ni+NTA SLS, around 3.3×10^{-8} mol of Ni are accumulated in the back resin at 24 hours,
400 in the mixed system, only 2.6×10^{-8} mol of Ni are accumulated in the back resin. This
401 implies that NiNTA is more inert in the mixed system than in the SLS, which supports
402 the computed lability values reported in Table 4.
403

404 ### 4.3.2 Metal accumulation

405 As mentioned above, both mixture and SLS experiments were made at the same
406 conditions of pH, ionic strength and bulk free ligand concentration (see Table 1 and
407 speciation compositions computed with Visual MINTEQ in Tables SI-1 and SI-2).
408 These conditions were chosen to meet three criteria: a) constant values of pH and ionic
409 strength ensure that kinetic constants are the same in SLS and mixture[31] (so, rate
410 constants fitted in the SLS can be used to predict accumulations in the mixture system);
411 b) any possible difference in the lability degree between SLS and mixture should only
412 be ascribed to specific mixture effects, and not to the effect of the bulk ligand
413 concentration (as discussed in Section 4.1.2 and Figure 1); and c) at least one of the
414 ligands in its free form (in this case, NTA) is present at a concentration comparable to
415 that of the metal (non-excess conditions).
416 The predicted accumulations in the mixture (at conditions listed in Table 1) are reported
417 in Table 4. As seen from a comparison with results listed in Table 2c, the relative error
418 $\left(\frac{\left|n_{\mathrm{Ni,exp}}-n_{\mathrm{Ni,sim}}\right|}{n_{\mathrm{Ni,exp}}}\right)$ of the numerical simulation in the Ni accumulation amounts to 10.1
419 % (8h), 16.3% (16h) and 7.0% (24h), which comprises possible experimental errors of
420 the accumulations measured in both the SLS and mixture systems, as well as any
421 uncertainty in the kinetic constants derived from the fitting to the SLS data.

As one of the main objectives of this work, these numerical simulation results were used to check the accuracy of the metal accumulations in the mixture predicted from values of $\xi_i^{h=1}$ instead of ξ_i . This procedure could be surprising since the above section has highlighted the differences between $\xi_i^{h=1}$ and ξ_i . Notice, however, that the variations of the individual lability degrees in the mixture (with respect to the SLS) are mutually opposite and tend to compensate each other when the total metal accumulation is considered. The advantage of $\xi_i^{h=1}$ is that this parameter is much more practical from an experimental point of view than ξ_i or even the use of the individual kinetic rate constants.

In the case of a mixed system made up with Ni, NTA and EN, Eqn. (7) turns into:

$$n_{\mathrm{Ni}} \approx At\left(\frac{D_{\mathrm{NiNTA}}c^{*}_{\mathrm{NiNTA}}}{\delta^{g}}\xi^{h=1}_{\mathrm{NiNTA}} + \frac{D^{\mathrm{eff}}_{\mathrm{NiEN}}c^{\mathrm{eff}\,*}_{\mathrm{NiEN}}}{\delta^{g}}\xi^{h=1}_{\mathrm{NiEN}^{\mathrm{eff}}}\right) \quad (28)$$

where the amount of free metal was assumed negligible, and effective species were used.

The results listed in Table 4 indicate that Eqn. (28) overestimates Ni accumulation with respect to the numerical simulation in: 11.5 % (8h), 10.7% (16h) and 10.4% (24h). These are, then, the percentage deviations due to non-additive effects in the mixture when the concentrations are those indicated in Table 1. The overestimation of the accumulation by Eqn. (28) agrees with the higher decrease in ξ_{NiNTA} with respect to $\xi^{h=1}_{\mathrm{NiNTA}}$ compared to the almost negligible increase in $\xi_{\mathrm{NiEN}^{\mathrm{eff}}}$, as seen in Figure 3.

It seems interesting to develop further the testing of Eqn. (28) to NTA:Ni concentration ratios other than that in Table 1 by using numerical simulation. The resulting theoretical accumulations are plotted in Figure 4, which shows that Eqn. (28) leads to values close

to (but below) simulation, with discrepancies at 24 hours lower than 11%, indicating moderate antagonistic effects of the mixture. These differences disappear at very low or high NTA concentrations, as expected, since the mixture tends to a SLS. These results support the fact that Eqn. (28) yields reasonable estimations of the metal accumulation in the mixture using the SLS values of the corresponding lability degrees, because, even though the actual values of the latter in the mixture deviate significantly from SLS, their variations tend to cancel out.

Although all natural systems are complex mixtures, mixture effects have not received until recently great interest. This work has focussed on the influence of the mixture composition on the metal availability measured with the DGT. In non-excess ligand conditions, complexes tend to become inert but they become even more inert in presence of a labile ligand. Thus, NiNTA complex has shown to be more inert after the addition of the labile EN ligand, *i.e.*, association of NiNTA is noticeably promoted by the presence of EN. This behaviour is the opposite of that found when both ligands are in excess. However, the effect of this influence on the total flux is limited for the Ni+NTA+en system. This work opens the way to analyse more complex systems and allows a deeper comprehension of what DGT is measuring.

Conflicts of interest

There are no conflicts of interest to declare

Acknowledgments

The authors gratefully acknowledge support for this research from the Spanish Ministry of Economy, Industry and Competitiveness MINECO (Project CTM2016-78798). The assistance of Federico Quattrini and Calin A. David is acknowledged.

5. Figures

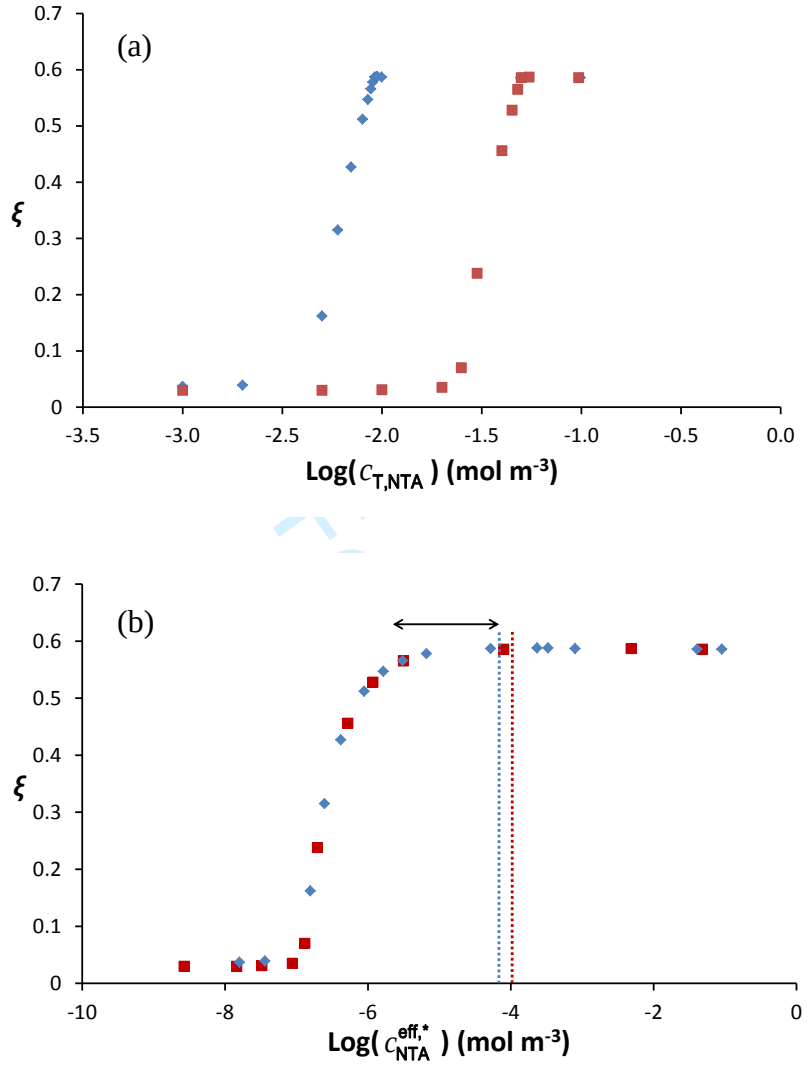

Figure 1. Lability degree, calculated with numerical simulation, of the complex NiNTA ($\xi_{NiNTA}^{h=1}$) in a single ligand system as a function of $c_{T,NTA}^{*}$ (panel a) or $c_{NTA}^{eff\,*}$ (panel b). Markers: $c_{T,Ni}^{*}$ =5×10^{-2} mol m^{-3} (red squares) and $c_{T,Ni}^{*}$ =9.2×10^{-3} mol m^{-3} (blue diamonds). Other parameters: $k_{d,NiNTA}^{eff}$ = 4.19 × 10^{-3} (s^{-1}), D_{Ni}= 6.09 × 10^{-10} m^{2} s^{-1}, $D_{NTA} = D_{NiNTA}$ = 4.75 × 10^{-10} m^{2} s^{-1}, δ^{r} =4×10^{-4} m, δ^{g} =1.1×10^{-3} m, $c_{T,R}$ =28 mol m^{-3}, t=10h and Π=2. High rate constants for the reaction between Ni and the resin sites have been used to obtain perfect-sink conditions. Vertical dotted lines stand for abscissae values corresponding to $c_{T,Ni}^{*} = c_{T,NTA}^{*}$.

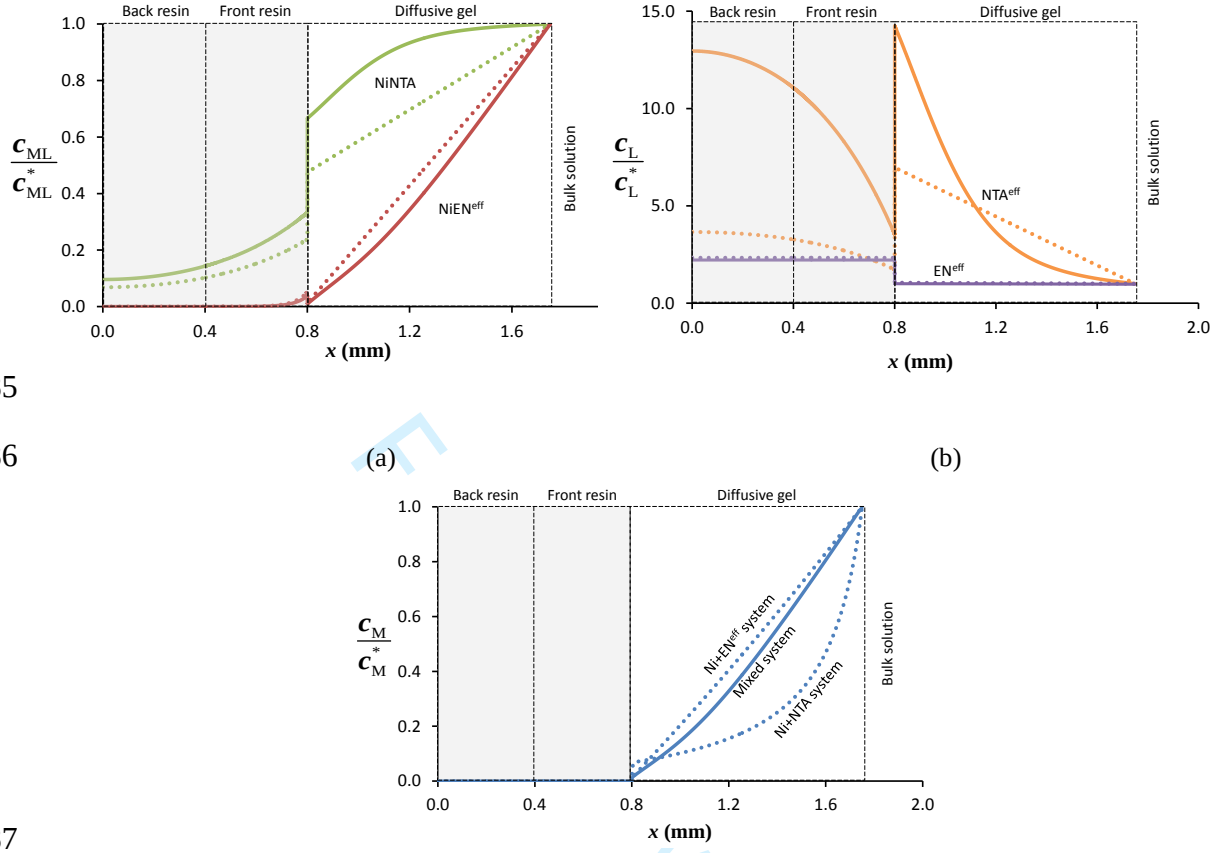

Figure 2. Normalized concentration profiles for (a) complexes, (b) ligands and (c) free Ni. Dotted lines stand for values in the SLS and continuous lines denote values in the mixed system. Parameters used: $c_{T,Ni}$ *= 2.3 ×10*$^{-2}$ *mol m*$^{-3}$, $c_{T,EN}$ *= 1.0 mol m*$^{-3}$, $c_{T,NTA}$ *= 10*$^{-2}$ *mol m*$^{-3}$, *pH=8.0, Ionic strength= 51 mol m*$^{-3}$. *The rest of parameters as in Figure 1.*

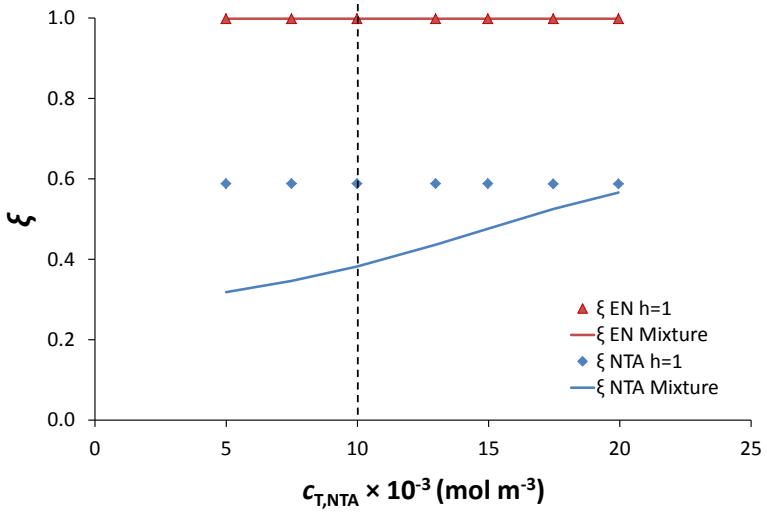

496 *Figure 3 Lability degree of the complexes (ξ) as a function of* $c_{T,NTA}$ for a solution
497 with $c^{*}_{T,Ni}$ *=2.3×10-2 mol m-3,* $c^{*}_{T,EN}$ *=1 mol m-3.Markers: triangles stand for the lability*
498 *of* $NiEN^{eff}$ *and diamonds for that of* $NiNTA$ *in a SLS. Continuous lines denote the*
499 *labilities of complexes in the mixed system. Vertical dashed line stand for* $c_{T,NTA}$ *= 10-2*
500 *mol m-3. Other parameters are gathered in Table 3. The rest, as in Figure 1.*
501

502

503

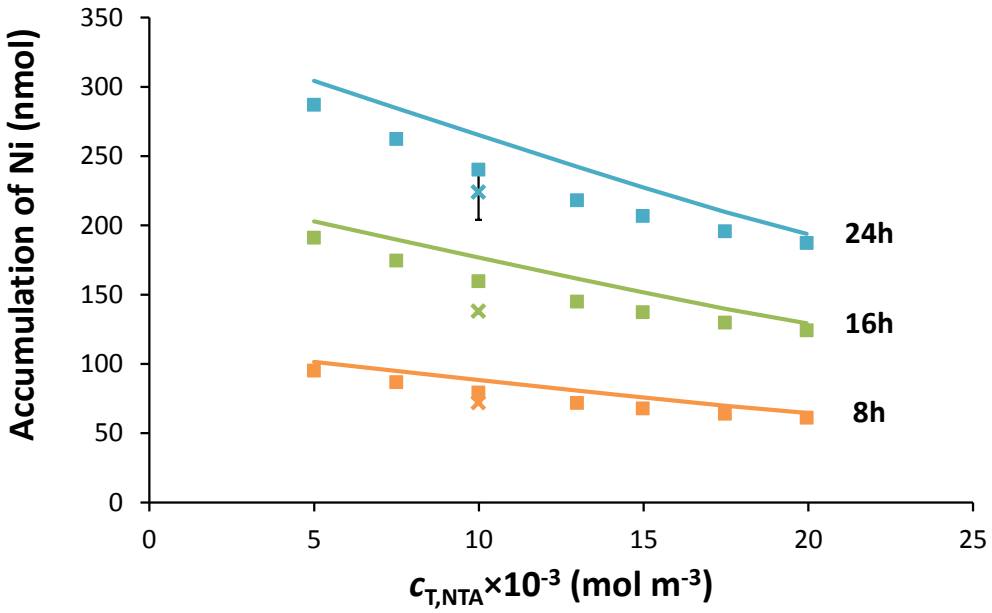

504

505 *Figure 4. Accumulation of Ni in the mixed ligand system as a function of total NTA*
506 *concentration. Markers: Squares stand for the accumulation of Ni calculated from*
507 *numerical simulation at 8h (orange), 16h (green) and 24h (blue). Cross:*
508 *experimental values measured at conditions specified in Table 1 for the*
509 *corresponding times. Continuous lines refer to accumulations derived using Eqn. 28.*
510 *Error bars refer to standard deviations. At t=8h and 16h error bars are so small that*
511 *overlap with the markers. Other parameters as in Figure 1.*
512

513

6. Tables

Table 1. Experimental conditions in the single ligand experiments and in the mixture (nominal values).

Parameters	Single ligand system (mol m^{-3})		Mixed ligand system (mol m^{-3})
	Ni + NTA	Ni + EN	
$c^*_{T,Ni}$	9.8×10^{-3}	2.5×10^{-2}	2.5×10^{-2}
$c^*_{T,NTA}$	10^{-2}	-	10^{-2}
$c^*_{T,EN}$	-	1	1
HEPES	1	1	1
I	50	50	50
pH	8.01 ± 0.01	8.00 ± 0.01	8.02 ± 0.02
T (ºC)	25	25	25

Table 2. Total accumulations of Ni (n_{Ni}), percentages of Ni accumulated in the back resin disc (%back) and lability degree measured in the single ligand systems. Conditions: pH=8.0 and Ionic strength= 51 mol m^{-3}. Panels: a) data corresponding to the single ligand system NiNTA. b) data corresponding to the single ligand system NiEN. c) data corresponding to the mixture. Concentrations are in each case those reported in Table 1.

a)

	SLS NiNTA system		
t (h)	**%back**	**n_{Ni} (nmol)**	**$\xi^{h=1}_{NiNTA}$**
8	39.7±4.7	23±3	0.60
16	40.8±0.7	40±1	
24	46.9±4.2	63±2	

b)

	SLS NiEN system		
t (h)	**%back**	**n_{Ni} (nmol)**	**$\xi^{h=1}_{NiEN^{eff}}$**
8	4.9±1.8	117±0.4	0.99
16	7.3±4.9	244±4	
24	3.9±0.3	362±9	

c)

	Mixture system Ni, NTA and EN	
***t* (h)**	**%back**	**n_{Ni} (nmol)**
8	13.3±1.4	72±0.5
16	15.4±1.9	138±2
24	11.6 ±1.8	224±14

Table 3. Effective kinetic and stability constants used in the simulation of the reactions with Ni, NTA and EN. Stability constants values have been left fixed to the values provided by Visual Minteq.

Reaction	$k^{eff}_{a,NiL}$ ($m^3 mol^{-1} s^{-1}$)	$k^{eff}_{d,NiL}$ (s^{-1})	K^{eff}_{NiL} ($m^3\ mol^{-1}$)
$Ni + NTA^{eff} \underset{k^{eff}_{d,NiNTA}}{\overset{k^{eff}_{a,NiNTA}}{\rightleftharpoons}} NiNTA^{eff}$	1.9×10^{6}	3.32×10^{-3}	5.72×10^{8}
$Ni + EN^{eff} \underset{k^{eff}_{d,NiEn}}{\overset{k^{eff}_{a,NiEn}}{\rightleftharpoons}} NiEN^{eff}$	8.41×10^{3}	3.54	2.37×10^{3}

Table 4. Prediction of the Ni accumulations for different times in the mixture described in Table 1. Labilities in the mixed system (ξ) of species $NiNTA$ and $NiEN^{eff}$ as computed with numerical simulation.

Time/h	**n_{Ni} (mol) Numerical simulation**	**n_{Ni} (mol) Using Eqn. (28)**	ξ_{NiNTA}	$\xi_{NiEN^{eff}}$
8	7.9×10^{-8}	8.8×10^{-8}	0.38	0.99
16	1.6×10^{-7}	1.7×10^{-7}		
24	2.4×10^{-7}	2.65×10^{-7}		

7. References

Reference List

1. Buffle, J. *Complexation Reactions in Aquatic Systems. An Analytical Approach.;* Ellis Horwood Limited: Chichester, 1988.

2. Fasfous, I. I.; Yapici, T.; Murimboh, J.; Hassan, I. M.; Chakrabarti, C. L.; Back, M. H.; Lean, D. R. S.; Gregoire, D. C. Kinetics of trace metal competition in the freshwater environment: Some fundamental characteristics. *Environ. Sci. Technol.* **2004,** *38* (19), 4979-4986.

3. Galceran, J.; van Leeuwen, H. P. Dynamics of biouptake processes: the role of transport, adsorption and internalisation. In *Physicochemical kinetics and transport at chemical-biological surfaces. IUPAC Series on Analytical and Physical Chemistry of Environmental Systems*, van Leeuwen, H. P., Koester, W., Eds.; John Wiley: Chichester (UK), 2004; Vol. 9, pp 147-203.

4. Alemani, D.; Buffle, J.; Zhang, Z.; Galceran, J.; Chopard, B. Metal flux and dynamic speciation at (bio)interfaces. Part IV: MHEDYN, a general code for metal flux computation; application to particulate complexants and their mixtures with the other natural ligands. *Environ. Sci. Technol.* **2008,** *42*, 2028-2033.

5. Buffle, J.; Wilkinson, K. J.; van Leeuwen, H. P. Chemodynamics and Bioavailability in Natural Waters. *Environ. Sci. Technol.* **2009,** *43* (19), 7170-7174.

6. Tusseau-Vuillemin, M. H.; Gilbin, R.; Bakkaus, E.; Garric, J. Performance of diffusion gradient in thin films to evaluate the toxic fraction of copper to Daphnia magna. *Environ. Toxicol. Chem.* **2004,** *23* (9), 2154-2161.

7. Galceran, J.; Puy, J.; Salvador, J.; Cecília, J.; van Leeuwen, H. P. Voltammetric lability of metal complexes at spherical microelectrodes with various radii. *J. Electroanal. Chem.* **2001,** *505* (1-2), 85-94.

8. Salvador, J.; Puy, J.; Cecilia, J.; Galceran, J. Lability of complexes in steady state finite planar diffusion. *J. Electroanal. Chem.* **2006,** *588*, 303-313.

9. Mota, A. M.; Pinheiro, J. P.; Goncalves, M. L. S. Electrochemical Methods for Speciation of Trace Elements in Marine Waters. Dynamic Aspects. *J. Phys. Chem. A* **2012,** *116* (25), 6433-6442.

10. Galceran, J.; Puy, J. Interpretation of diffusion gradients in thin films (DGT) measurements: a systematic approach. *Environ. Chem.* **2015,** *12* (2), 112-122.

11. van Leeuwen, H. P.; Town, R. M.; Buffle, J.; Cleven, R.; Davison, W.; Puy, J.; van Riemsdijk, W. H.; Sigg, L. Dynamic speciation analysis and Bioavailability of metals in Aquatic Systems. *Environ. Sci. Technol.* **2005,** *39*, 8545-8585.

12. Galceran, J.; Puy, J.; Salvador, J.; Cecília, J.; Mas, F.; Garcés, J. L. Lability and mobility effects on mixtures of ligands under steady-state conditions. *Phys. Chem. Chem. Phys.* **2003,** *5*, 5091-5100.

13. Salvador, J.; Garcés, J. L.; Companys, E.; Cecilia, J.; Galceran, J.; Puy, J.; Town, R. M. Ligand mixture effects in metal complex lability. *J. Phys. Chem. A* **2007,** *111* (20), 4304-4311.

14. Salvador, J.; Garcés, J. L.; Galceran, J.; Puy, J. Lability of a mixture of metal complexes under steady-state planar diffusion in a finite domain. *J. Phys. Chem. B* **2006,** *110* (27), 13661-13669.

15. Pinheiro, J. P.; Salvador, J.; Companys, E.; Galceran, J.; Puy, J. Experimental verification of the metal flux enhancement in a mixture of two metal complexes: the Cd/NTA/glycine and Cd/NTA/citric acid systems. *Phys. Chem. Chem. Phys.* **2010,** *12* (5), 1131-1138.

16. Zhang, Z. S.; Buffle, J. Interfacial Metal Flux in Ligand Mixtures. 1. The Revisited Reaction Layer Approximation: Theory and Examples of Applications. *J. Phys. Chem. A* **2009,** *113* (24), 6562-6571.

17. Zhang, Z. S.; Buffle, J.; Town, R. M.; Puy, J.; van Leeuwen, H. P. Metal Flux in Ligand Mixtures. 2. Flux Enhancement Due to Kinetic Interplay: Comparison of the Reaction Layer Approximation with a Rigorous Approach. *J. Phys. Chem. A* **2009,** *113* (24), 6572-6580.

18. Davison, W.; Zhang, H.; Grime, G. W. PERFORMANCE-CHARACTERISTICS OF GEL PROBES USED FOR MEASURING THE CHEMISTRY OF PORE WATERS. *Environ. Sci. Technol.* **1994,** *28* (9), 1623-1632.

19. Zhang, H.; Davison, W. Performance characteristics of diffusion gradients in thin films for the insitu measurement of trace metals in aqueous solution. *Anal. Chem.* **1995,** *67* (19), 3391-3400.

20. Mongin, S.; Uribe, R.; Puy, J.; Cecilia, J.; Galceran, J.; Zhang, H.; Davison, W. Key Role of the Resin Layer Thickness in the Lability of Complexes Measured by DGT. *Environ. Sci. Technol.* **2011,** *45* (11), 4869-4875.

21. Uribe, R.; Mongin, S.; Puy, J.; Cecilia, J.; Galceran, J.; Zhang, H.; Davison, W. Contribution of Partially Labile Complexes to the DGT Metal Flux. *Environ. Sci. Technol.* **2011,** *45* (12), 5317-5322.

22. Puy, J.; Uribe, R.; Mongin, S.; Galceran, J.; Cecilia, J.; Levy, J.; Zhang, H.; Davison, W. Lability Criteria in Diffusive Gradients in Thin Films. *J. Phys. Chem. A* **2012,** *116* (25), 6564-6573.

23. Uribe, R.; Puy, J.; Cecilia, J.; Galceran, J. Kinetic Mixture Effects in Diffusion Gradients in Thin Films (DGT). *Phys. Chem. Chem. Phys.* **2013,** *15* (27), 11349-11355.

24. Puy, J.; Galceran, J.; Rey-Castro, C. *Diffusive gradients in thin-films for environmental measurements;* Cambridge ed.; 2017.pp. 93-122.

25. Bayen, S.; Wilkinson, K. J.; Buffle, J. The permeation liquid membrane as a sensor for free nickel in aqueous samples. *The Analyst* **2007,** *132*, 262-267.

26. Ferreira, C. M. H.; Pinto, I. S. S.; Soares, E. V.; Soares, H. M. V. M. (Un)suitability of the use of pH buffers in biological, biochemical and environmental studies and their interaction with metal ions - a review. *Rsc Advances* **2015,** *5* (39), 30989-31003.

27. *Visual MINTEQ version 3.1. https://vminteq.lwr.kth.se/download/,* 2016

28. Shiva, A. H.; Teasdale, P. R.; Bennett, W. W.; Welsh, D. T. A systematic determination of diffusion coefficients of trace elements in open and restricted diffusive layers used by the diffusive gradients in a thin film technique. *Anal. Chim. Acta* **2015,** *888*, 146-154.

29. Scally, S.; Davison, W.; Zhang, H. Diffusion coefficients of metals and metal complexes in hydrogels used in diffusive gradients in thin films. *Anal. Chim. Acta* **2006,** *558* (1-2), 222-229.

30. Mongin, S.; Uribe, R.; Rey-Castro, C.; Cecilia, J.; Galceran, J.; Puy, J. Limits of the Linear Accumulation Regime of DGT Sensors. *Environ. Sci. Technol.* **2013,** *47*, 10438-10445.

31. Puy, J.; Galceran, J.; Cruz-Gonzalez, S.; David, C. A.; Uribe, R.; Lin, C.; Zhang, H.; Davison, W. Metal accumulation in DGT: Impact of ionic strength and kinetics of dissociation of complexes in the resin domain. *Anal. Chem.* **2014,** *86*, 7740-7748.

32. Shafaei-Arvajeh, M. R.; Lehto, N.; Garmo, O. A.; Zhang, H. Kinetic Studies of Ni Organic Complexes Using Diffusive Gradients in Thin Films (DGT) with Double Binding Layers and a Dynamic Numerical Model. *Environ. Sci. Technol.* **2013,** *47* (1), 463-470.

33. Fatin-Rouge, N.; Milon, A.; Buffle, J.; Goulet, R. R.; Tessier, A. Diffusion and partitioning of solutes in agarose hydrogels: The relative influence of electrostatic and specific interactions. *J. Phys. Chem. B* **2003,** *107* (44), 12126-12137.

34. van der Veeken, P. L. R.; van Leeuwen, H. P. Gel-water partitioning of soil humics in diffusive gradient in thin film (DGT) analysis of their metal complexes. *Environ. Chem.* **2012,** *9* (1), 24-30.

35. Huang, J. Y.; Bennett, W. W.; Welsh, D. T.; Li, T. L.; Teasdale, P. R. "Diffusive Gradients in Thin Films" Techniques Provide Representative Time-Weighted Average Measurements of Inorganic Nutrients in Dynamic Freshwater Systems. *Environmental Science & Technology* **2016,** *50* (24), 13446-13454.

36. Sangi, M. R.; Halstead, M. J.; Hunter, K. A. Use of the diffusion gradient thin film method to measure trace metals in fresh waters at low ionic strength. *Anal. Chim. Acta* **2002,** *456* (2), 241-251.

665 37. Golmohamadi, M.; Davis, T. A.; Wilkinson, K. J. Diffusion and Partitioning of
666 Cations in an Agarose Hydrogel. *J. Phys. Chem. A* **2012,** *116* (25), 6505-
667 6510.

668 38. Puy, J.; Cecília, J.; Galceran, J.; Town, R. M.; van Leeuwen, H. P. Voltammetric
669 lability of multiligand complexes. The case of ML_2. *J. Electroanal. Chem.*
670 **2004,** *571* (2), 121-132.
671
672

SUPPLEMENTARY MATERIAL

Mixture of ligands influence on metal accumulation in Diffusive Gradients in Thin films (DGT)

Alexandra Altier[a], Martín Jiménez[a], Ramiro Uribe[c], Carlos Rey-Castro[a], Joan Cecília[b], Josep Galceran[a], Jaume Puy[a*]

[a]*Departament de Química.* [b]*Departament de Matemàtica. Universitat de Lleida, and AGROTECNIO, Rovira Roure 191, 25198 Lleida, Spain.*

* Phone number: 34 973 702529. Email address: jpuy@quimica.udl.cat

Table of Contents

1. Experimental systems

Experiments at nominal elemental concentrations reported in Table 1 of the main text for Ni, NTA and EN in separate or mixed systems were done at pH 8 and salt background 50 mol·m^{-3}. Current concentrations in the bulk solution were determined with ICP-MS measurements. Values are reported in Table SI-1

Table SI-1. Ni concentrations measured in the bulk solution of the single ligand experiments and in the mixture with ICP-MS.

Parameters	**Single ligand systems (mol m^{-3})**		**Mixed ligand system (mol m^{-3})**
	Ni + NTA	**Ni + EN**	
$C^*_{T,Ni}$	9.2×10^{-3}	2.4×10^{-2}	2.3×10^{-2}
$C^*_{T,NTA}$	10^{-2}	-	10^{-2}
$C^*_{T,EN}$	-	1	1
HEPES	1	1	1
I	50	50	50
pH	8.01 ± 0.01	8.00 ± 0.01	8.02 ± 0.02
***T* (ºC)**	25	25	25

Once these concentrations are used as input values in Visual MINTEQ, speciation results reported in Tables SI-2 and SI-3 are obtained.

Table SI-2. Percentage of the species formed in single and mixed ligand system under experimental conditions specified in Table SI-1.

Component	**% of total concentration**			**Species name**
	Single ligand system NiNTA	**Single ligand system NiEN**	**Mixed ligand system**	
Ni^{2+}	0.016	0.041	0.022	Ni^{2+}
	-	6.893	3.881	NiEN
	-	84.454	48.634	$Ni(EN)_2$
	-	8.607	5.069	$Ni(EN)_3$
	99.84	-	42.344	$NiNTA^-$

	0.051	-	-	$Ni(NTA)_2^{4-}$
	0.09	-	0.038	$NiOHNTA^{2-}$
EN	-	0.8	0.818	EN
NTA^{3-}	0.106	-	0.033	NTA^{3-}

Table SI-3. Speciation in SLS and in the mixture under the experimental conditions specified in Table SI-1, using the speciation program Visual MINTEQ.

	SLS NiNTA (mol m^{-3})	**SLS NiEN (mol m^{-3})**	**Mixture (mol m^{-3})**
CO_3^{2-}	5.94×10^{-3}	5.96×10^{-3}	5.96×10^{-3}
EN	-	8.00×10^{-3}	8.18×10^{-3}
HEN	-	8.37×10^{-1}	8.56×10^{-1}
H^+	1.22×10^{-5}	1.22×10^{-5}	1.22×10^{-5}
H_2EN	-	1.07×10^{-1}	1.09×10^{-1}
$H_2CO_3^*$ (aq)	1.28×10^{-2}	1.28×10^{-2}	1.28×10^{-2}
H_2NTA^-	3.88×10^{-9}	-	1.18×10^{-9}
H_3NTA (aq)	3.15×10^{-15}	-	9.54×10^{-16}
H_4NTA^+	3.88×10^{-22}	-	1.18×10^{-22}
HCO^{3-}	7.00×10^{-1}	7.00×10^{-1}	7.00×10^{-1}
$HEPES^-$	7.71×10^{-1}	7.71×10^{-1}	7.71×10^{-1}
H-HEPES (aq)	2.29×10^{-1}	2.29×10^{-1}	2.29×10^{-1}
$HNTA^{2-}$	7.95×10^{-4}	-	2.42×10^{-4}
Na^+	$4.95\times10^{+1}$	$4.95\times10^{+1}$	$4.95\times10^{+1}$
$NaCO^{3-}$	2.48×10^{-3}	2.48×10^{-3}	2.48×10^{-3}
$NaHCO_3$ (aq)	1.16×10^{-2}	1.15×10^{-2}	1.15×10^{-2}
$NaNO_3$ (aq)	4.60×10^{-1}	4.59×10^{-1}	4.60×10^{-1}
$NaNTA^{2-}$	1.14×10^{-5}	-	3.45×10^{-6}
NaOH (aq)	5.08×10^{-5}	5.08×10^{-5}	5.08×10^{-5}
$Ni(NTA)_2^{4-}$	4.82×10^{-6}	-	1.58×10^{-6}
$Ni(OH)_2$ (aq)	6.65×10^{-10}	4.41×10^{-9}	2.33×10^{-9}
$Ni(OH)_3^-$	8.24×10^{-13}	5.47×10^{-12}	2.89×10^{-12}
NiEN	-	1.65×10^{-3}	8.93×10^{-4}
$Ni(EN)_2$	-	2.03×10^{-2}	1.12×10^{-2}

$Ni(EN)_3$	-	2.07×10^{-3}	1.17×10^{-3}
Ni^{+2}	1.47×10^{-6}	9.78×10^{-6}	5.16×10^{-6}
$NiCO_3$ (aq)	6.59×10^{-8}	4.37×10^{-7}	2.30×10^{-7}
$NiHCO^{3+}$	5.75×10^{-8}	3.82×10^{-7}	2.01×10^{-7}
$NiNO^{3+}$	8.29×10^{-8}	5.50×10^{-7}	2.90×10^{-7}
$NiNTA^{-}$	9.17×10^{-3}	-	9.74×10^{-3}
$NiOH^{+}$	1.03×10^{-8}	6.82×10^{-8}	3.60×10^{-8}
$NiOHNTA^{2-}$	8.30×10^{-6}	-	8.84×10^{-6}
NO_3^{-}	$4.95\times10^{+1}$	$4.96\times10^{+1}$	$4.96\times10^{+1}$
NTA^{3-}	1.09×10^{-5}	-	3.32×10^{-6}
OH^{-}	1.22×10^{-3}	1.23×10^{-3}	1.23×10^{-3}
NTA^{eff}	8.17×10^{-4}	-	2.49×10^{-4}
EN^{eff}	-	9.52×10^{-1}	9.73×10^{-1}

Total concentrations were chosen to reach, in equilibrium, a negligible free metal concentration and to ensure that the accumulation is only due to the complex contribution. The effects of the mixture on the lability degree are then expected to be more noticeable. Moreover, pH 8 was selected since it leads to a free Ni concentration in the mixed system smaller than 1% of the total Ni concentration (See Table SI-1). A free Ni concentration corresponding to 3.9 % of the total is, for instance, predicted at pH 7.

The lability degree of a given complex species changes in the presence of a mixture of ligands[1]. The change is more evident for partially labile complexes which can vary on both directions (increasing or decreasing lability)[2]. We have, then, included a partially labile complex in the mixture. Indeed, at ionic strength 50 mol m^{-3}, the complex NiNTA shows a partially labile behaviour[3] and the complex NiEN has a labile behaviour[4] .

Concentrations of the different solutions have been selected to keep common bulk concentrations of free metal, complex and free ligand in the mixture and in the corresponding SLS. We aim at using $\xi_i^{h=1}$ values as surrogates of ξ_i in the mixture and

assessing the accuracy of this estimation of the metal accumulation in the mixtures. As seen in Table SI-3, due to the experimental random errors, total concentrations used in the SLS do not lead to common bulk concentrations of free metal, complex and ligand than in the mixture. For instance, the NTA^{eff} concentration in the SLS is close to three times the concentrations that it has in the mixture. An important part of this difference comes from the small change between the nominal concentrations indicated in Table 1 of the main text and those in the bulk solution measured by ICP-MS (Table SI-1) as can be confirmed with the speciation prediction of VMINTEQ.

According to the values in Table SI-3, neglecting the ionic pairs, the desired values of total Ni and total NTA in the SLS are 9.745×10^{-3} and 9.989×10^{-3} mol·m^{-3}, respectively instead of those found in Table SI-1. These small differences do not modify $\xi^{h=1}_{\mathrm{NiNTA}}$, since the condition $c^{*}_{\mathrm{T,NTA}} > 0.625 c^{*}_{\mathrm{T,Ni}}$ (indicated in Section 3.1.1 of the main text as a rough estimation of the minimum $c^{*}_{\mathrm{T,NTA}}$ that ensures that the lability degree of the NiNTA is that of the excess of ligand conditions) is fulfilled by both the actual SLS concentrations reported in Table SI-1 and those reported in this paragraph.

For the NiEN system, the differences between the free EN^{eff} concentration in the SLS and in the mixture increase. However, no effects are expected from this change, since EN^{eff} is in excess of ligand conditions where the lability degree has been shown to be almost independent of the ligand concentration.

1.1 DGT deployment procedure

DGT pistons and cap mouldings were cleaned overnight where the following sequence was always assumed:they were soaked in 2% phosphate-free, surface-active detergent called DECON-90 supplied by Decon Laboratories Limited, Sussex, UK. Afterwards, they remained in Milli-Q water at least one day. At that point,hey were washed with Milli-Q water until bubbles disappeared. [5] Then, they were cleaned using four 1 h 10%

nitric acid (Analytical Reagent Grade, Fisher Chemical) soaks. Finally, they were rinsed with Milli-Q water until the pH is around 5.

Prior to the serial-time deployments, the assembled DGT samples were immersed for at least 18 hours in a pre-conditioning solution with the same pH and ionic strength as the test solution.

A 5 L polyethylene container, pre-cleaned by using three 24 h 10% HNO_3 soaks, was thermostated at 25 ± 0.1 °C controlled by a thermostatic bath where the test solution container was introduced and was stirred at 240 rpm using an overhead stirrer. To provide a well-stirred solution (to ensure that the diffusive boundary layer ,DBL, thickness is negligible compared with the total thickness summation of the filter and diffusive gel thickness [6-8]), the solution was stirred continuously. Prior to deploying the DGT samplers in 2 L of test solution, the solution was stirring for at least 24 hours to equilibrate and the pH was adjusted to the desired value by adding diluted HNO_3 or NaOH as explained above. pH was measured during the deployment of the DGT sensors using a pH meter Orion 920+ (Thermo electron Corporation). Three sets of triplicate DGT sensors were deployed in the solutions and retrieved after 8, 16 and 24 hours. 1 mL aliquots of the test solution were taken at regular intervals of time to control the total amount of metal. After deployment, the DGT samples were retrieved and then rinsed with Milli-Q water, the fitted cap was removed, and the resin layers were carefully placed into 1.5 mL micro-centrifuge PVC tubes. Metals were eluted from retrieved membranes by immersing them in 1 mL of 20% HNO_3 for at least 24 hours to allow an efficient metal extraction from the resin.

Samples were diluted 50-fold and deployment solutions and metal accumulations were analyzed by inductively coupled plasma mass spectrometry (ICP-MS, 7700 Series, Agilent).

The mass of the metal accumulated in the resin was calculated as,

$$n = c_e(V_e + V_g) / f_e \quad \text{(SI.1)}$$

where n is the amount of metal accumulated in the resin, c_e is the concentration from ICP-MS measurements of the eluted resin gel (mol m^{-3}), V_e is the eluent volume, V_g is the resin gel volume and f_e is the elution factor, in this case 1[9].

1.2 DGT accumulations

Accumulation results are shown in Figure SI-1 and SI-2 for SLS and Figure SI-3 for the mixture.

Table SI-4. Total experimental accumulation of Ni and back percentage for different deployment times for SLS and mixed ligand system.

	SLS NiNTA		**SLS NiEN**		**Mixed ligand system**	
Time (h)	**n_T (nmol)**	**%back**	**n_T (nmol)**	**%back**	**n_T (nmol)**	**%back**
8	23	40	117	5	72	13
16	40	41	244	7	138	15
24	63	47	362	4	224	12

The accumulated mass of Ni in devices with two resin layers, labelled front (F) and back (B), was converted to concentration by using Eqn. (SI.1) and values of diffusion coefficients reported in the main text. Values are expressed as ratios of amount of metal (nmol) over bulk concentration to refer the measurement to a fixed metal concentration avoiding dilution effects.

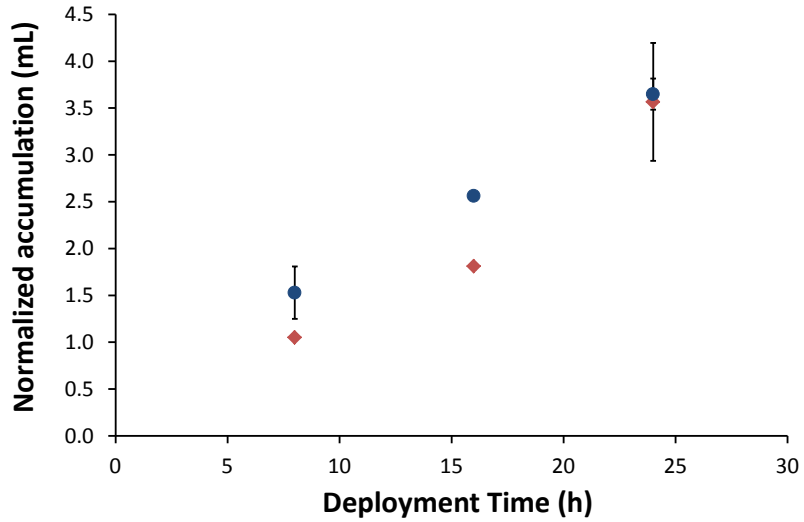

Figure SI-1. Time-series of DGT normalized accumulation (nmol/c) in a SLS NiNTA in the front (red bullet) and in the back (blue diamond) at 25 ºC. Experimental conditions as mentioned in Table SI-1. Error bars refer to standard deviations.*

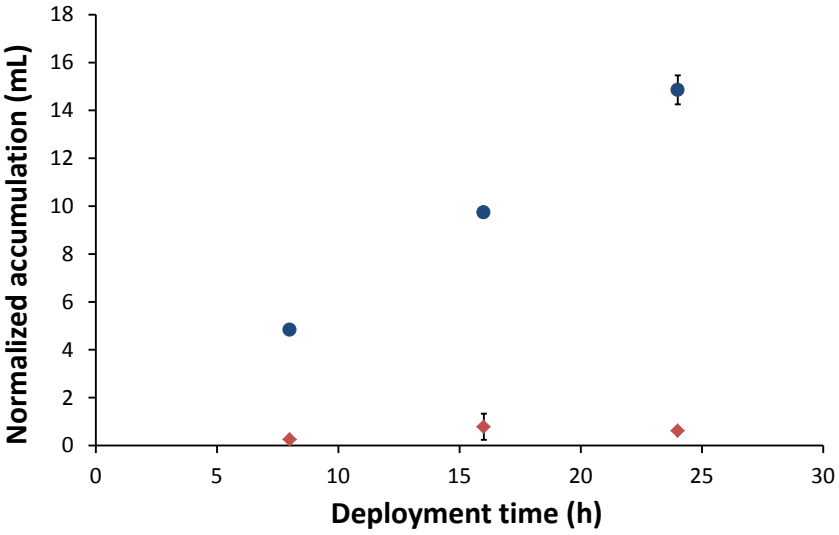

Figure SI-2. Time-series of DGT normalized accumulation (nmol/c) in a SLS NiEN in the front (red bullet) and in the back (blue diamond) at 25 ºC. Experimental conditions as mentioned in Table SI-1. Error bars refer to standard deviations.*

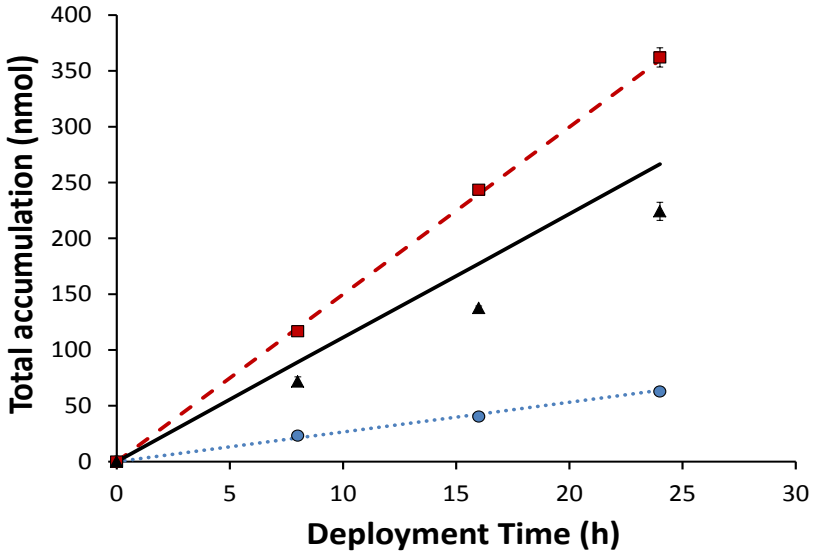

Figure SI-3. Time evolution of the total accumulation of Ni in DGT devices with two resin discs. Markers correspond to experimental accumulations of Ni in SLS NiNTA (blue circle), SLS NiEN (red square) and in the mixed ligand system (black triangle). Dashed line corresponds to Ni accumulation assuming perfect-sink conditions for SLS NiEN. Dotted line corresponds to Ni accumulation assuming perfect-sink conditions for SLS NiNTA. Continuous line corresponds to the Ni accumulation using the values obtained from Eq. 28 in the main text. Experimental conditions as mentioned in Table SI-1 for each experiment. Error bars refer to standard deviations.

Table SI-5 . Normalized accumulation of Ni (accumulated moles over the bulk concentration) in DGT devices with two resin gels after 8, 16 and 24 h deployment normalized by bulk solutions in single ligand systems. Experimental conditions are reported in Table SI-1.

Time (h)	sensor	$n_{Ni}^{only\ NTA} / c_{T,Ni}^{*}$ (mL)	$n_{Ni}^{only\ EN} / c_{T,Ni}^{*}$ (mL)
8	**F**	1.53 ± 0.28	4.84 ± 0.14
	B	1.05 ± 0.01	0.25 ± 0.10
	% Back	39.77 ± 4.77	4.90 ± 1.76
16	**F**	2.56 ± 0.03	9.74 ± 0.18
	B	1.81 ± 0.03	0.78 ± 0.55
	% Back	40.79 ± 0.70	7.31 ± 4.95
24	**F**	3.65 ± 0.17	14.86 ± 0.61
	B	3.57 ± 0.63	0.61 ± 0.03
	% Back	46.97 ± 4.23	3.91 ± 0.30

2. General Mathematical Formulation

For the range of concentrations used in this work, the relevant complexation reactions of Ni with NTA are:

$$\mathrm{Ni} + \mathrm{NTA} \underset{k_{d,\mathrm{NiNTA}}}{\overset{k_{a,\mathrm{NiNTA}}}{\rightleftharpoons}} \mathrm{NiNTA} \quad \text{(SI.2)}$$

$$\mathrm{H} + \mathrm{NTA} \underset{k_{d,\mathrm{HNTA}}}{\overset{k_{a,\mathrm{HNTA}}}{\rightleftharpoons}} \mathrm{HNTA} \quad \text{(SI.3)}$$

and the relevant complexation reactions of Ni with EN are:

$$\mathrm{Ni} + \mathrm{EN} \underset{k_{d,\mathrm{NiEN}}}{\overset{k_{a,\mathrm{NiEN}}}{\rightleftharpoons}} \mathrm{NiEN} \quad \text{(SI.4)}$$

$$\mathrm{NiEN} + \mathrm{EN} \underset{k_{d,\mathrm{Ni(EN)_2}}}{\overset{k_{a,\mathrm{Ni(EN)_2}}}{\rightleftharpoons}} \mathrm{Ni(EN)_2} \quad \text{(SI.5)}$$

$$\mathrm{Ni(EN)_2} + \mathrm{EN} \underset{k_{d,\mathrm{Ni(EN)_3}}}{\overset{k_{a,\mathrm{Ni(EN)_3}}}{\rightleftharpoons}} \mathrm{Ni(EN)_3} \quad \text{(SI.6)}$$

$$\mathrm{H} + \mathrm{EN} \underset{k_{d,\mathrm{HEN}}}{\overset{k_{a,\mathrm{HEN}}}{\rightleftharpoons}} \mathrm{HEN} \quad \text{(SI.7)}$$

$$\mathrm{H} + \mathrm{HEN} \underset{k_{d,\mathrm{H_2EN}}}{\overset{k_{a,\mathrm{H_2EN}}}{\rightleftharpoons}} \mathrm{H_2EN} \quad \text{(SI.8)}$$

Additionally, the reaction of Ni with the Chelex beads in the resin domain has also to be considered:

$$\mathrm{Ni} + \mathrm{R} \underset{k_{d,\mathrm{NiR}}}{\overset{k_{a,\mathrm{NiR}}}{\rightleftharpoons}} \mathrm{NiR} \quad \text{(SI.9)}$$

Full mathematical formulation for the SLS or the mixture has been done by writing the pertaining reaction-diffusion equations. Boundary conditions include bulk concentrations at the diffusive gel/bulk solution interface and flux null at the bottom of the resin domain corresponding to x=0. Continuity of the flux of each species has been considered at the resin diffusive gel interface. Numerical solution of the resulting system can be achieved with the simulation tool especially written to analyse mixture systems and described in the SI of [10,11]. Finite Element Method is used for the solution of the spatial dependence, while Finite Differences are used for the temporal dependence.

In order to include in the simulation the effect of the buffer to keep pH constant, reaction-diffusion equations for a buffer (HA) have also been considered. Thus additional species, HA, A and H have been introduced at concentrations high enough to keep pH constant and equal to the desired value (bulk concentrations of HA, A and H are 81.7, 18.3 and 10^{-5} mol m^{-3}, respectively).

3. Fitting the experimental accumulations

For the simulations, it was assumed that the diffusion coefficients of ligands, protonated ligands and complexes are equal. The value of the diffusion coefficient of Ni was taken from [12]. For species involved in the buffer reaction (H, A, HA), the value for the diffusion coefficient was assumed very high, in comparison with the values for other species, to have an homogeneous pH value. Values for these coefficients are presented in Table SI-6.

Table SI-6. Diffusion coefficients of species used in simulations

Species	D (m^2 s^{-1})
Ni	6.08×10^{-10}
NTA, NiNTA, HNTA	4.75×10^{-10}
EN, NiEN, $Ni(EN)_2$, $Ni(EN)_3$, HEN, H_2EN	6.08×10^{-10}
H, A, HA	1.00×10^{-8}

Migration effects were considered using the partition model explained in [10]. The Boltzmann factor was measured experimentally as explained in the main manuscript. For I=0.051 mol L^{-1}, a value of $\Pi = 2.0$ was used in simulations.

Stability constants for reactions (SI.2) - (SI.8) were obtained from Visual MINTEQ 3.1.

Assuming that the formation/dissociation of NiEN is the rate limiting step in the stepwise complexation, the kinetic rate constants for the formation/dissociation of

$Ni(EN)_2$ and $Ni(EN)_3$ were selected high enough to neglect their influence in the results, but keeping the ratio $k_{a,Ni(EN)_i}/k_{d,Ni(EN)_i}$ equal to the equilibrium constant $K_{Ni(EN)_i}$.

Additionally, all the protonation reactions are assumed to be fast enough to reach equilibrium instantaneously, so that the acid base equilibrium relationships apply.

Appropriate values for the kinetic constants ($k_{a,NiNTA}$ and $k_{d,NiNTA}$) were selected to fit the Ni accumulations for the single NiNTA system presented in Table SI-8. Experimental and calculated accumulations for the fitted values of the kinetic constants are reported in Table SI-8a.

The system NiEN is almost fully labile. Accordingly, the accumulation is almost independent of the particular kinetic constant $k_{d,NiEN}$ and the lowest value approaching the accumulation within a 2% discrepancy was selected. Additionally, the stability constant reported in Visual MINTEQ was used. Experimental and calculated accumulations for the fitted values of the kinetic constants are reported in Table SI-8b.

The kinetic and the stability constants for the reaction of Ni with the resin sites appearing in Eqn. (SI.9) were assumed high enough to simulate perfect sink conditions.

The set of parameters used in the complexation reactions NiNTA, NiEN and NiR are gathered in Table SI-7.

Table SI-7. Kinetic and stability constants for reactions used in simulations for systems with Ni, NTA and EN.

Reaction	k_a ($m^3 mol^{-1} s^{-1}$)	k_d (s^{-1})	K ($m^3 mol^{-1}$)
$Ni + NTA \underset{k_{d,NiNTA}}{\overset{k_{a,NiNTA}}{\rightleftharpoons}} NiNTA$	1.90×10^{6}	3.32×10^{-3}	5.72×10^{8}
$H + NTA \underset{k_{d,HNTA}}{\overset{k_{a,HNTA}}{\rightleftharpoons}} HNTA$	7.29×10^{6}	1.00	7.29×10^{6}
$Ni + EN \underset{k_{d,NiEN}}{\overset{k_{a,NiEN}}{\rightleftharpoons}} NiEN$	1.00×10^{6}	46.9	2.13×10^{4}

$NiEN + EN \underset{k_{d,Ni(EN)_2}}{\overset{k_{a,Ni(EN)_2}}{\rightleftharpoons}} Ni(EN)_2$	1.53×10^{3}	1.00	1.53×10^{3}
$Ni(EN)_2 + EN \underset{k_{d,Ni(EN)_3}}{\overset{k_{a,Ni(EN)_3}}{\rightleftharpoons}} Ni(EN)_3$	12.7	1.00	12.74
$H + EN \underset{k_{d,HEN}}{\overset{k_{a,HEN}}{\rightleftharpoons}} HEN$	1.05×10^{7}	1.00	1.05×10^{7}
$H + HEN \underset{k_{d,H_2EN}}{\overset{k_{a,H_2EN}}{\rightleftharpoons}} H_2EN$	1.28×10^{4}	1.00	1.28×10^{4}
$H + A \underset{k_{d,HA}}{\overset{k_{a,HA}}{\rightleftharpoons}} HA$	4.47×10^{5}	1.00	4.47×10^{5}
$Ni + R \underset{k_{d,NiR}}{\overset{k_{a,NiR}}{\rightleftharpoons}} NiR$	10^{15}	1.00	10^{15}

Table SI-8. Total accumulation of Ni and back percentage for different deployment times for panel a) SLS NiNTA and panel b) SLS NiEN obtained experimentally and by simulation.

a)

	SLS NiNTA			
Time (h)	$n_{T,exp}$ **(nmol)**	**%back$_{exp}$**	$n_{T,\,calc}$ **(nmol)**	**%back, calc**
8	23	40	21	30
16	40	41	42	30
24	63	47	62	30

b)

	SLS NiEN			
Time (h)	$n_{T,exp}$ **(nmol)**	**%back$_{exp}$**	$n_{T,\,calc}$ **(nmol)**	**%back, calc**
8	117	5	119	0
16	244	7	238	0
24	362	4	357	0

4. Formulation of the NiNTA and NiEN systems in terms of only one complex species.

A general scheme of the volume reactions in the systems NiNTA and NiEN is:

$$\begin{array}{ccccccc} \mathrm{M}+\mathrm{L} & \underset{k_{\mathrm{d},1}}{\overset{k_{\mathrm{a},1}}{\rightleftharpoons}} & \mathrm{ML} & +\mathrm{L} \underset{k_{\mathrm{d},2}}{\overset{k_{\mathrm{a},2}}{\rightleftharpoons}} & \mathrm{ML_2}+\mathrm{L} \underset{k_{\mathrm{d},3}}{\overset{k_{\mathrm{a},3}}{\rightleftharpoons}} & \mathrm{ML_3}+\mathrm{L} \\ & & + & & & & \\ & & \mathrm{H} & & & & \\ & & k_{\mathrm{d\_H},1} \uparrow\downarrow k_{\mathrm{a\_H},1} & & & & \\ & & \mathrm{HL} & & & & \\ & & + & & & & \\ & & \mathrm{H} & & & & \\ & & k_{\mathrm{d\_H},2} \uparrow\downarrow k_{\mathrm{a\_H},2} & & & & \\ & & .... & & & & \\ & & \mathrm{H_4L} & & & & \end{array} \qquad \text{(SI.10)}$$

where M stands for Ni while L stands for either NTA or EN. $k_{\mathrm{a},j}$ and $k_{\mathrm{d},j}$ label the association and dissociation rate constants, respectively.

Eqn. (SI.10) indicates that the metal can form different complex species of different M:L stoichiometric ratios which is the case of the reaction of Ni with EN, while L is also involved in acid-base equilibria, which applies to both NTA and EN.

We assume that i) the formation/dissociation of ML is the rate limiting step in the stepwise complexation of the metal M with the ligand L so that ML_2 and ML_3 can be instantaneously related to ML through the equilibrium relationships and ii) all the protonation reactions are fast enough to reach equilibrium instantaneously so that the acid base equilibrium relationships apply:

$$K_{\mathrm{H},i} = \frac{c_{\mathrm{H}_i\,\mathrm{L}}}{c_{\mathrm{H}}^{i}\; c_{\mathrm{H}_{(i-1)}\,\mathrm{L}}} \qquad \text{I4 (SI.11)}$$

Under these conditions, defining the bound metal, c_{M_b}, as:

$$c_{\mathrm{M}_b} = c_{\mathrm{ML}} + c_{\mathrm{ML}_2} + c_{\mathrm{ML}_3} \qquad \text{(SI.12)}$$

and $c_{\mathrm{L}}^{\mathrm{eff}}$ as an effective concentration of ligand corresponding to all the ligand species without metal bound,

$$c_{\mathrm{L}}^{\mathrm{eff}} = c_{\mathrm{L}} + c_{\mathrm{HL}} + c_{\mathrm{H_2L}} + c_{\mathrm{H_3L}} + c_{\mathrm{H_4L}} \qquad \text{(SI.13)}$$

a closed system of differential reaction-diffusion equations for c_{M}, c_{M_b} and $c_{\mathrm{L}}^{\mathrm{eff}}$ can be written as[13]:

$$\frac{\partial c_{\mathrm{M}}}{\partial t} = D_{\mathrm{M}} \frac{\partial^2 c_{\mathrm{M}}}{\partial x^2} + \frac{k_{\mathrm{d},1}}{1 + \frac{K_2 c_{\mathrm{L}}^{\mathrm{eff}}}{B} + \frac{K_2 K_3 \left(c_{\mathrm{L}}^{\mathrm{eff}}\right)^2}{B^2}} c_{\mathrm{M}_b} - \frac{k_{\mathrm{a},1}}{B} c_{\mathrm{M}} c_{\mathrm{L}}^{\mathrm{eff}} \qquad \text{(SI.14)}$$

$$\frac{\partial c_{\mathrm{M}_b}}{\partial t} = \left(\frac{D_{\mathrm{ML}} + D_{\mathrm{ML}_2} \frac{K_2 c_{\mathrm{L}}^{\mathrm{eff}}}{B}}{1 + \frac{K_2 c_{\mathrm{L}}^{\mathrm{eff}}}{B} + \frac{K_2 K_3 \left(c_{\mathrm{L}}^{\mathrm{eff}}\right)^2}{B^2}} \right) \frac{\partial^2 c_{\mathrm{M}_b}}{\partial x^2} - \frac{k_{\mathrm{d},1}}{1 + \frac{K_2 c_{\mathrm{L}}^{\mathrm{eff}}}{B} + \frac{K_2 K_3 \left(c_{\mathrm{L}}^{\mathrm{eff}}\right)^2}{B^2}} c_{\mathrm{M}_b} + \frac{k_{\mathrm{a},1}}{B} c_{\mathrm{M}} c_{\mathrm{L}}^{\mathrm{eff}} \qquad \text{(SI.15)}$$

and

$$\frac{\partial c_{\mathrm{L}}^{\mathrm{eff}}}{\partial t} = D_{\mathrm{L}} \frac{\partial^2 c_{\mathrm{L}}^{\mathrm{eff}}}{\partial x^2} + \frac{k_{\mathrm{d},1}}{1 + \frac{K_2 c_{\mathrm{L}}^{\mathrm{eff}}}{B} + \frac{K_2 K_3 \left(c_{\mathrm{L}}^{\mathrm{eff}}\right)^2}{B^2}} c_{\mathrm{M}_b} - \frac{k_{\mathrm{a},1}}{B} c_{\mathrm{M}} c_{\mathrm{L}}^{\mathrm{eff}} \qquad \text{(SI.16)}$$

where D_i stands for the diffusion coefficient of species i,

$$B = 1 + K_{\mathrm{H},1} c_{\mathrm{H}} + K_{\mathrm{H},1} K_{\mathrm{H},2} c_{\mathrm{H}}^2 + K_{\mathrm{H},1} K_{\mathrm{H},2} K_{\mathrm{H},3} c_{\mathrm{H}}^3 + K_{\mathrm{H},1} K_{\mathrm{H},2} K_{\mathrm{H},3} K_{\mathrm{H},4} c_{\mathrm{H}}^4 \qquad \text{(SI.17)}$$

$$K_i = \frac{k_{a,i}}{k_{d,i}} \qquad \text{(SI.18)}$$

and $K_{\mathrm{H},i}$ stand for the association acid constants as indicated in Eqn. (SI.11).

Equations (SI.12) to (SI.16) are formally identical to a system with one ligand with concentration $c_{\mathrm{L}}^{\mathrm{eff}}$, that is not involved in any protonation and formation of multiple equilibria with the metal, whenever the system is in excess of ligand conditions and a buffer or a fast enough diffusion of the protons ensures a homogenous concentration profile for c_{H}. Indeed, only under these conditions the effective association and dissociation constants of this metal to ligand effective reaction are constant and given by:

$$k_{\mathrm{a}}^{\mathrm{eff}} = \frac{k_{\mathrm{a},1}}{B} \qquad \text{I12(SI.19)}$$

$$k_{\mathrm{d}}^{\mathrm{eff}} = \frac{k_{\mathrm{d},1}}{1+\frac{K_2 c_{\mathrm{L}}^{\mathrm{eff}}}{B}+\frac{K_2 K_3 \left(c_{\mathrm{L}}^{\mathrm{eff}}\right)^2}{B^2}} \tag{SI.20}$$

The effective stability constant of the metal complexation with this formal ligand $c_{\mathrm{L}}^{\mathrm{eff}}$ is:

$$K^{\mathrm{eff}} = \frac{k_{\mathrm{a}}^{\mathrm{eff}}}{k_{\mathrm{d}}^{\mathrm{eff}}} = \frac{K_1\left(1+\frac{K_2 c_{\mathrm{L}}^{\mathrm{eff}}}{B}+\frac{K_2 K_3 \left(c_{\mathrm{L}}^{\mathrm{eff}}\right)^2}{B^2}\right)}{B} \tag{SI.21}$$

The effective diffusion coefficients of the effective species are given by:

$$D_{\mathrm{ML}}^{\mathrm{eff}} = \frac{D_{\mathrm{ML}} + D_{\mathrm{ML}_2}\frac{K_2 c_{\mathrm{L}}^{\mathrm{eff}}}{B} + D_{\mathrm{ML}_3}\frac{K_2 c_{\mathrm{L}}^{\mathrm{eff}}}{B}\frac{K_3 c_{\mathrm{L}}^{\mathrm{eff}}}{B}}{1+\frac{K_2 c_{\mathrm{L}}^{\mathrm{eff}}}{B}+\frac{K_2 c_{\mathrm{L}}^{\mathrm{eff}}}{B}\frac{K_3 c_{\mathrm{L}}^{\mathrm{eff}}}{B}} \tag{SI.22}$$

and

$$D_{\mathrm{L}}^{\mathrm{eff}} = D_{\mathrm{L}} \tag{SI.23}$$

4.1 The case of NiNTA

Equations (SI.19)-(SI.22) for the NiNTA SLS become:

$$k_{\mathrm{a,NiNTA}}^{\mathrm{eff}} = \frac{k_{\mathrm{a,NiNTA}}}{1+K_{\mathrm{HNTA}} c_{\mathrm{H}}} \tag{SI.24}$$

$$k_{\mathrm{d,NiNTA}}^{\mathrm{eff}} = k_{\mathrm{d,NiNTA}} \tag{SI.25}$$

$$K_{\mathrm{NiNTA}}^{\mathrm{eff}} = \frac{k_{\mathrm{a,NiNTA}}^{\mathrm{eff}}}{k_{\mathrm{d,NiNTA}}^{\mathrm{eff}}} = \frac{K_{\mathrm{NiNTA}}}{1+K_{\mathrm{HNTA}} c_{\mathrm{H}}} \tag{SI.26}$$

$$c_{\mathrm{NTA}}^{\mathrm{eff}} = c_{\mathrm{NTA}} + c_{\mathrm{HNTA}} \tag{SI.27}$$

and

$$D_{\mathrm{NTA}}^{\mathrm{eff}} = D_{\mathrm{NTA}} \tag{SI.28}$$

The use of these effective parameters allows to rewrite the processes described in Eqns. (SI.2)-(SI.3) as only one process:

$$\mathrm{Ni} + \mathrm{NTA}^{\mathrm{eff}} \underset{k^{\mathrm{eff}}_{\mathrm{d,NiNTA}}}{\overset{k^{\mathrm{eff}}_{\mathrm{a,NiNTA}}}{\rightleftharpoons}} \mathrm{NiNTA} \tag{SI.29}$$

being $k^{\mathrm{eff}}_{\mathrm{a,NiNTA}}$ a real constant because H/OH diffuse faster than the rest of ions diffusivity and we use a buffer to keep pH constant.

4.2 The case of NiEN

For the effective complexation process

$$\mathrm{Ni} + \mathrm{EN}^{\mathrm{eff}} \underset{k^{\mathrm{eff}}_{\mathrm{d,NiEN}}}{\overset{k^{\mathrm{eff}}_{\mathrm{a,NiEN}}}{\rightleftharpoons}} \mathrm{NiEN}^{\mathrm{eff}} \tag{SI.30}$$

Equations (SI.19)-(SI.22) become:

$$k^{\mathrm{eff}}_{\mathrm{a,NiEN}} = \frac{k_{\mathrm{a,NiEN}}}{B} \tag{SI.31}$$

$$k^{\mathrm{eff}}_{\mathrm{d,NiEN}} = \frac{k_{\mathrm{d,NiEN}}}{1 + \dfrac{K_{\mathrm{Ni(EN)_2}} c^{\mathrm{eff}}_{\mathrm{EN}}}{B}} \tag{SI.32}$$

$$B = 1 + K_{\mathrm{HEN}} c_{\mathrm{H}} + K_{\mathrm{HEN}} K_{\mathrm{H_2EN}} c^2_{\mathrm{H}} \tag{SI.33}$$

$$K^{\mathrm{eff}}_{\mathrm{NiEN}} = \frac{k^{\mathrm{eff}}_{\mathrm{a,NiEN}}}{k^{\mathrm{eff}}_{\mathrm{d,NiEN}}} \tag{SI.34}$$

with:

$$c^{\mathrm{eff}}_{\mathrm{EN}} = c_{\mathrm{EN}} + c_{\mathrm{HEN}} + c_{\mathrm{H_2EN}} \tag{SI.35}$$

$$c^{\mathrm{eff}}_{\mathrm{NiEN}} = c_{\mathrm{NiEN}} + c_{\mathrm{Ni(EN)_2}} + c_{\mathrm{Ni(EN)_3}} \tag{SI.36}$$

Eqns. (SI.31)-(SI.34) indicate that $k^{\mathrm{eff}}_{\mathrm{a,NiEN}}$ and $k^{\mathrm{eff}}_{\mathrm{d,NiEN}}$ are only constant parameters, independent on the spatial position, whenever the concentration profile of $c^{\mathrm{eff}}_{\mathrm{EN}}$ is homogenous in addition to that of c_{H}. The use of the buffer and the high diffusion coefficient of H ensures the homogeneity of c_{H}. Excess of ligand conditions support a

homogeneous profile of c_{EN}^{eff}. Thus, Equations (SI.31)-(SI.34) can be applied to the NiEN system allowing to rewrite the full system as a set of equations formally equivalent to a system with only one reaction, Eqn. (SI.30).

These effective species allow us to more easily understand the mixing effect, analyzing the concentration profiles, as shown in the main manuscript.

5. Dependence of the lability degree on the ligand concentration in a single ligand system

The dependence of the lability degree on the ligand concentration is especially important for weak complexes, which tend to be labile in excess of ligand conditions and can become almost inert in non-excess of ligand conditions. Lability of strong complexes shows a more moderate dependence on the ligand concentration, since they tend to be already inert or partially labile even in excess of ligand conditions. Figure SI-4a shows the dependence of the lability degree with the ligand concentration, for different values of the complex stability constant. Figure SI-4b shows how the relative contribution of the complex to the overall metal accumulation decays with decreasing ligand concentration, while the total metal accumulation rises due to the decreasing ratio of complex and free metal concentrations in bulk solution. The accumulation reaches a maximum value when there is no metal complexed in bulk solution and all the metal is transported to the resin as free metal.

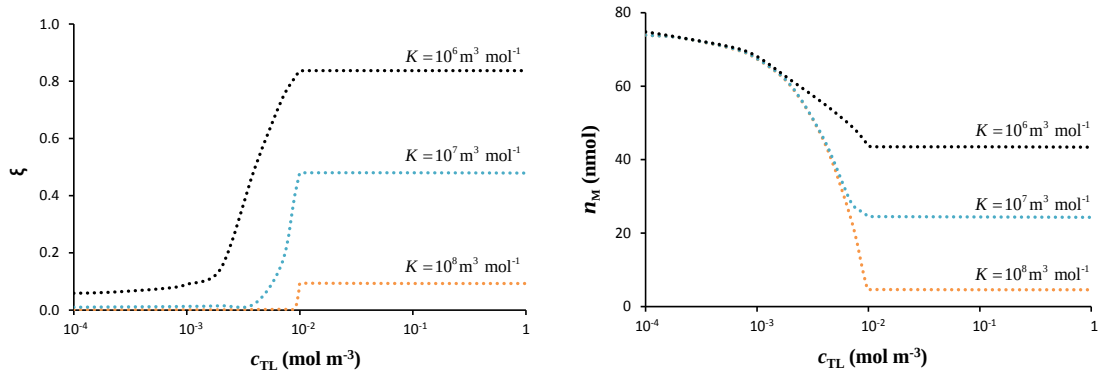

(a) (b)

Figure SI-4. Lability degree of the complex (ξ) and total accumulation of metal (n_M) as functions of c_{TL} in a single ligand system. Results obtained using numerical simulation for different values of stability constant. Parameters used: c_{TM} = 10^{-2} mol m^{-3}, D_M = 6.09 × 10^{-10} m^2 s^{-1}, D_L = 4.26 × 10^{-10} m^2 s^{-1}, D_{ML} = 4.26 × 10^{-10} m^2 s^{-1}, δ^r =4×10^{-4} m, δ^g =1.1×10^{-3} m, $c_{T,R}$ =28 mol m^{-3}, k_a =10^4 m^3 mol^{-1} s^{-1}, t=10h. Perfect-sink conditions between M and the resin sites have been used.

6. Dependence of the metal accumulation on the stoichiometry of MEN complex

Table SI-9. Percentage of the species formed in the system MEN and moles of metal normalised with bulk concentration accumulated by DGT in a system with EN concentration of 0.01 mol L^{-1} and 10^{-5} mol L^{-1} Co, Cu, Cd and Zn and 2.5 × 10^{-5} mol L^{-1}, I=6.2 mol m^{-3} at pH 9.

Component	% of total concentration	Species name	Accumulated nmol/c^* (mL)
Ni^{+2}	7.805	$Ni(EN)_2$	15.34
	92.189	$Ni(EN)_3$	
Cd^{+2}	3.189	CdEN	15.83
	92.45	$Cd(EN)_2$	
	4.347	$Cd(EN)_3$	
Co^{+2}	45.29	$Co(EN)_2$	10.50
	53.492	$Co(EN)_3$	
	1.213	CoEN	
Zn^{+2}	0.424	ZnEN	16.94
	34.669	$Zn(EN)_2$	
	64.897	$Zn(EN)_3$	
Cu^{+2}	100	$Cu(EN)_2$	15.83

References

Reference List

1. Uribe, R.; Puy, J.; Cecilia, J.; Galceran, J. Kinetic Mixture Effects in Diffusion Gradients in Thin Films (DGT). *Phys. Chem. Chem. Phys.* **2013,** *15* (27), 11349-11355.

2. Salvador, J.; Garcés, J. L.; Companys, E.; Cecilia, J.; Galceran, J.; Puy, J.; Town, R. M. Ligand mixture effects in metal complex lability. *J. Phys. Chem. A* **2007,** *111* (20), 4304-4311.

3. Puy, J.; Galceran, J.; Cruz-Gonzalez, S.; David, C. A.; Uribe, R.; Lin, C.; Zhang, H.; Davison, W. Metal accumulation in DGT: Impact of ionic strength and kinetics of dissociation of complexes in the resin domain. *Anal. Chem.* **2014,** *86*, 7740-7748.

4. Sara Cruz-González Availability of metal ions and ZnO nanoparticles in aqueous media. University of Lleida, 2014.

5. *Diffusive Gradients in Thin-Films for Environmental Measurements.;* Cambridge University Press: Cambridge (UK), 2016.

6. Garmo, O. A.; Naqvi, K. R.; Royset, O.; Steinnes, E. Estimation of diffusive boundary layer thickness in studies involving diffusive gradients in thin films (DGT). *Anal. Bioanal. Chem.* **2006,** *386* (7-8), 2233-2237.

7. Warnken, K. W.; Zhang, H.; Davison, W. Accuracy of the diffusive gradients in thin-films technique: Diffusive boundary layer and effective sampling area considerations. *Anal. Chem.* **2006,** *78* (11), 3780-3787.

8. Zhang, H.; Davison, W. Performance characteristics of diffusion gradients in thin films for the insitu measurement of trace metals in aqueous solution. *Anal. Chem.* **1995,** *67* (19), 3391-3400.

9. Mongin, S. Contributions to the study of the availability of metal ions in aquatic systems. PhD thesis. Universitat de Lleida., Jul 2012.

10. Altier, A.; Jimenez-Piedrahita, M.; Rey-Castro, C.; Cecilia, J.; Galceran, J.; Puy, J. Accumulation of Mg to Diffusive Gradients in Thin Films (DGT) Devices: Kinetic and Thermodynamic Effects of the Ionic Strength. *Anal. Chem.* **2016,** *88* (20), 10245-10251.

11. Jimenez-Piedrahita, M.; Altier, A.; Cecilia, J.; Rey-Castro, C.; Galceran, J.; Puy, J. Influence of the settling of the resin beads on Diffusion Gradients in Thin films measurements. *Anal. Chim. Acta* **2015,** *885*, 148-155.

12. Shiva, A. H.; Teasdale, P. R.; Bennett, W. W.; Welsh, D. T. A systematic determination of diffusion coefficients of trace elements in open and restricted diffusive layers used by the diffusive gradients in a thin film technique. *Anal. Chim. Acta* **2015,** *888*, 146-154.

13. Mongin, S.; Uribe, R.; Rey-Castro, C.; Cecilia, J.; Galceran, J.; Puy, J. Limits of the Linear Accumulation Regime of DGT Sensors. *Environ. Sci. Technol.* **2013,** *47*, 10438-10445.